Study of the process $e^+e^- \to \pi^+\pi^-\pi^0$ using ISR at BaBar

Vladimir Druzhinin, Evgeny Kozyrev, Evgeny Solodov

BINP, Novosibirsk

Introduction

The process $e^+e^- \to \pi^+\pi^-\pi^0$ gives the second largest contribution into $a_\mu^{\text{had,LO-VP}}$ and its error.

$a_\mu^{\text{had,LO-VP}}$

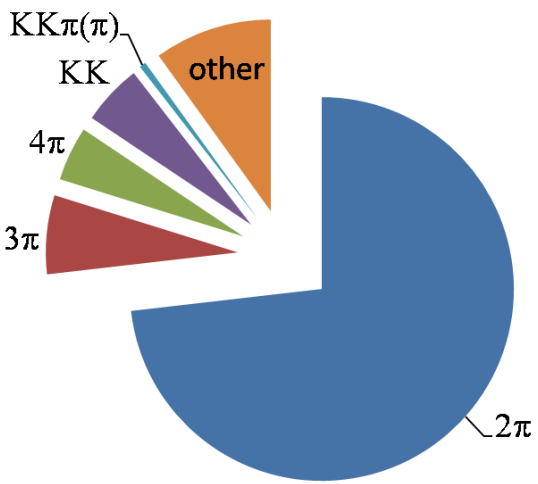

$a_\mu^{\text{had,LO-VP}}$ error squared

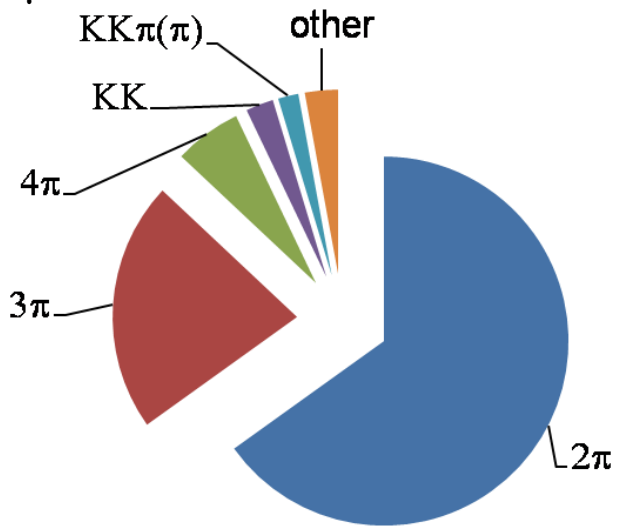

- ✓ Currently the $e^+e^- \to \pi^+\pi^-\pi^0$ contribution is known with about 3% accuracy
- ✓ We plan to improve this accuracy to 1.5%.

Existing measurement

- VEPP-2M (Novosibirsk): SND (0.66-1.4 GeV), CMD-2 (ω and ϕ regions)
- BABAR (1.05-3 GeV), fit to the 3π mass spectrum below 1.05 GeV
- SND@VEPP-2000 1.05-2 GeV, Dalitz plot analysis → observation $\omega(1650)\to\rho(1450)\pi$

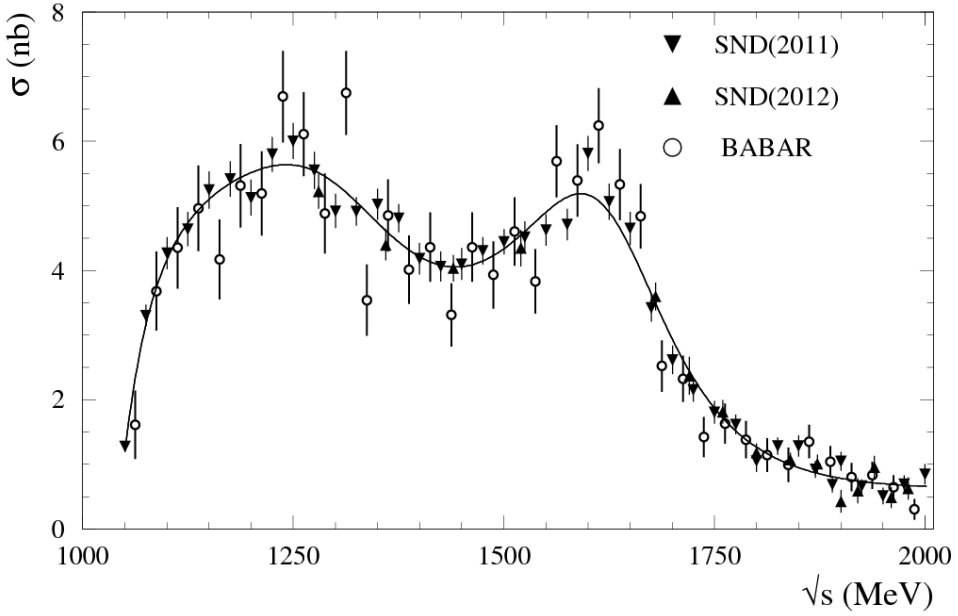

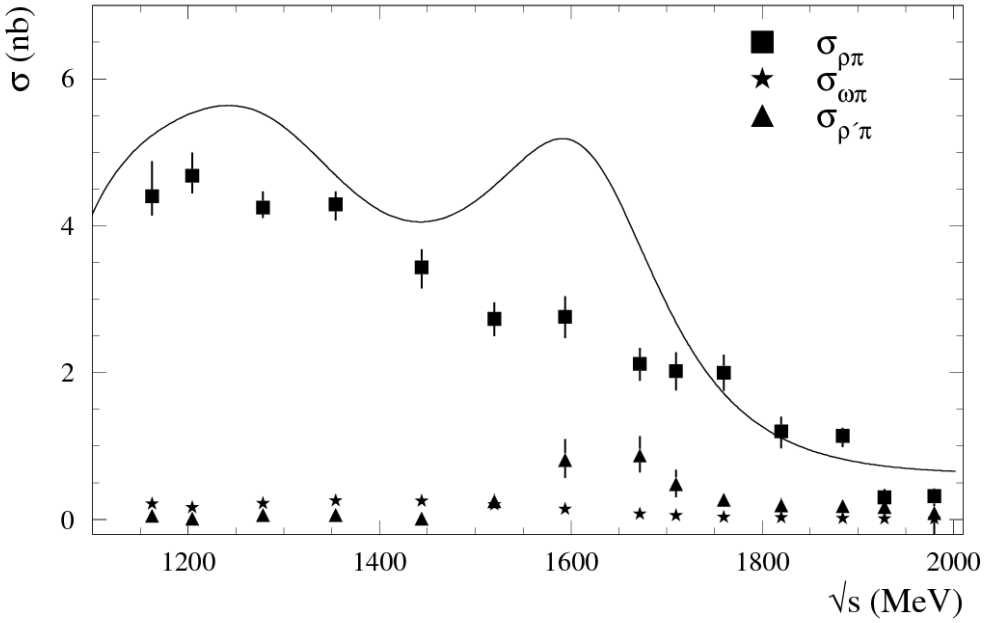

Existing measurements

- Large (8%=2σ) difference between SND+BABAR and CMD-2 measurements of the $\omega(782)$ peak cross section
- BES-III (arXiv:1912.11208) confirms a larger (SND+BABAR) value of the $\omega(782)$ peak cross section, measures $a_\mu^{3\pi}$ with 1.1% accuracy.
- Future measurements
  - BABAR
  - SND
  - CMD-3

ISR method

$$\frac{d\sigma(s,x)}{dx\,d(\cos\theta)} = W(s,x,\theta)\cdot\sigma_0\big(s(1-x)\big),$$

$$W(s,x,\theta) = \frac{\alpha}{\pi x}\left(\frac{2-2x+x^2}{\sin^2\theta} - \frac{x^2}{2}\right),\quad x = \frac{2E_\gamma}{\sqrt{s}}$$

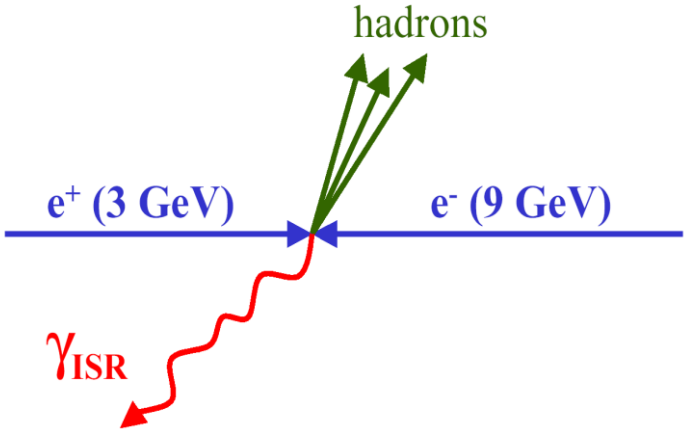

The mass spectrum of the hadronic system in the reaction $e^+e^- \to X+\gamma$ is related to the cross section for the nonradiative process $e^+e^- \to X$.

At BABAR the measurement of the cross section at low energies (below 2.5 GeV) can be performed in the tagged mode, with detection of the ISR photon.

Selection of $e^+e^- \to \pi^+\pi^-\pi^0$ candidate events

- Two charged particles with p_T>50 MeV/c originated from the interaction region. $23° < \theta_\pi < 140°$
- ISR photon candidate with $E_{\gamma,cm}$>3 GeV. $23° < \theta_\gamma < 137.5°$
- π^0 candidate: two photons with E_γ>100 MeV with invariant mass in the 100-170 MeV range. $23° < \theta_\gamma < 137.5°$
- Kinematic fit with requirements of energy and momentum balance and mass constraint for the π^0 candidate.
  - Standard selection - χ^2<40
  - Tight selection - χ^2<20

Kinematic fit χ^2

- Points – data
- Open histogram – simulation
- Green histogram – calculated background

The tight selection is used for cross section measurement.

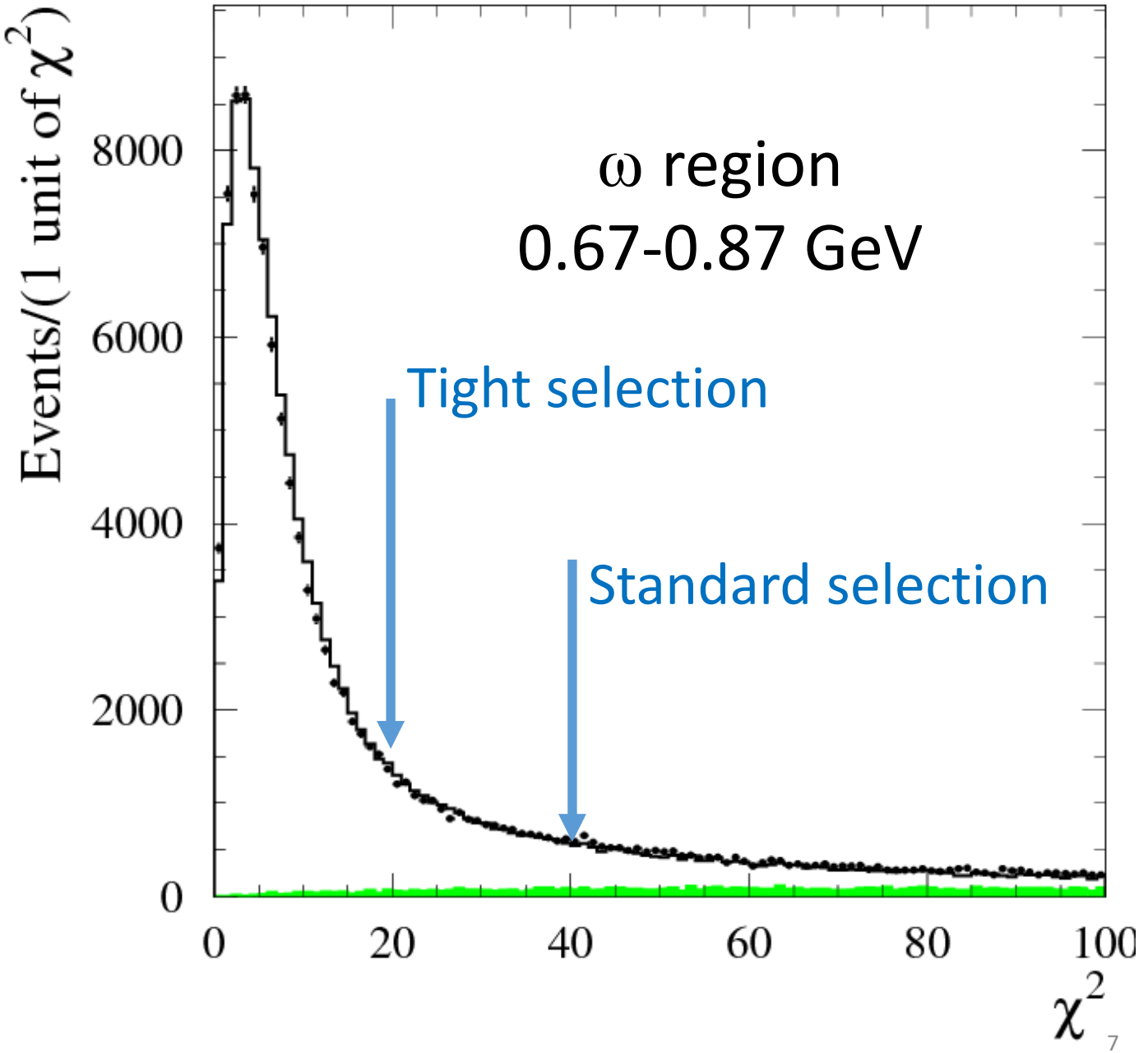

Background sources

- ISR processes
  - $e^+e^- \to e^+e^-\gamma$
  - $e^+e^- \to \pi^+\pi^-\pi^0\pi^0\gamma$
  - $e^+e^- \to \pi^+\pi^-\gamma$
  - $e^+e^- \to K^+K^-\pi^0\gamma$
  - …
- Non-ISR processes
  - $e^+e^- \to q\bar{q}$, in particular $e^+e^- \to \pi^+\pi^-\pi^0\pi^0$
  - $e^+e^- \to \tau^+\tau^-$

Background suppression

1. Several conditions at different stages against $e^+e^- \to e^+e^-\gamma$. None of the charged tracks is identified as an electron.
2. None of the charged tracks is identified as a kaon ($K^+K^-\pi^0\gamma$)
3. $E_{\pi^0} > 0.4$ GeV ($\pi^+\pi^-\gamma, \mu^+\mu^-\gamma$)
4. Mass recoiling against $\pi^+\pi^-$ pair squared is larger than 5 GeV^2 ($\pi^+\pi^-\gamma, \mu^+\mu^-\gamma, \pi^+\pi^-\pi^0\pi^0$)
5. $\chi^2_{4\pi\gamma} > 30$ ($\pi^+\pi^-\pi^0\pi^0\gamma$)
6. $M^*_{\gamma\gamma}$ is the invariant mass of two photons, one of which is the ISR photon candidate, while the second has E_γ>100 MeV. Events with $0.1 < M^*_{\gamma\gamma} < 0.17$ GeV are rejected ($\pi^+\pi^-\pi^0\pi^0$)
7. $M_{\pi\gamma} > 1.5$ GeV, where $M_{\pi\gamma}$ is the invariant mass of the the ISR photon candidate and one of the charged pions ($\tau^+\tau^-, \pi^+\pi^-\pi^0\pi^0$)

Background suppression

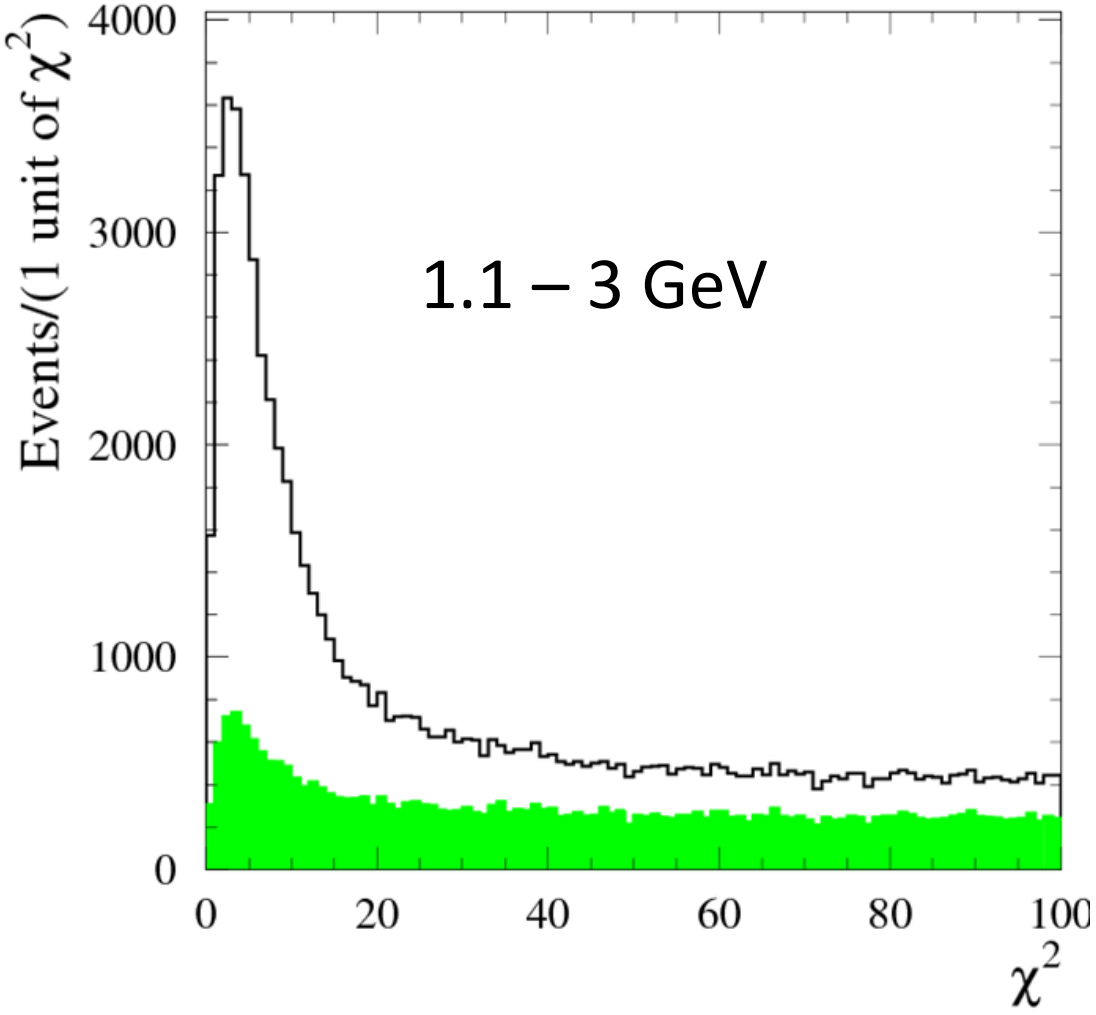

- The green histogram shows events rejected by the background suppression cuts in the region 1.1-3 GeV.
- The fraction of background events is decreased by a factor of 2.5 with loss of signal events of 15-17%.
- Below 1.1 GeV the background is small. Its fraction is 2% (1%) with the standard (tight) selection.

Background estimation

- ✓ The most important ISR background processes $e^+e^- \to \pi^+\pi^-\pi^0\pi^0\gamma$, $e^+e^- \to \pi^+\pi^-\gamma$, $e^+e^- \to K^+K^-\pi^0\gamma$ are normalized using data.
- ✓ The contributions of other ISR processes are estimated using MC simulation reweighed according to existing cross section measurements.
- ✓ To estimate the $e^+e^- \to \pi^+\pi^-\pi^0\pi^0$ and non-4π $q\bar{q}$ contributions, events from the π^0 peak in the $M^*_{\gamma\gamma}$ distribution are analyzed.

Background normalization, $e^+e^- \to K^+K^-\pi^0\gamma$

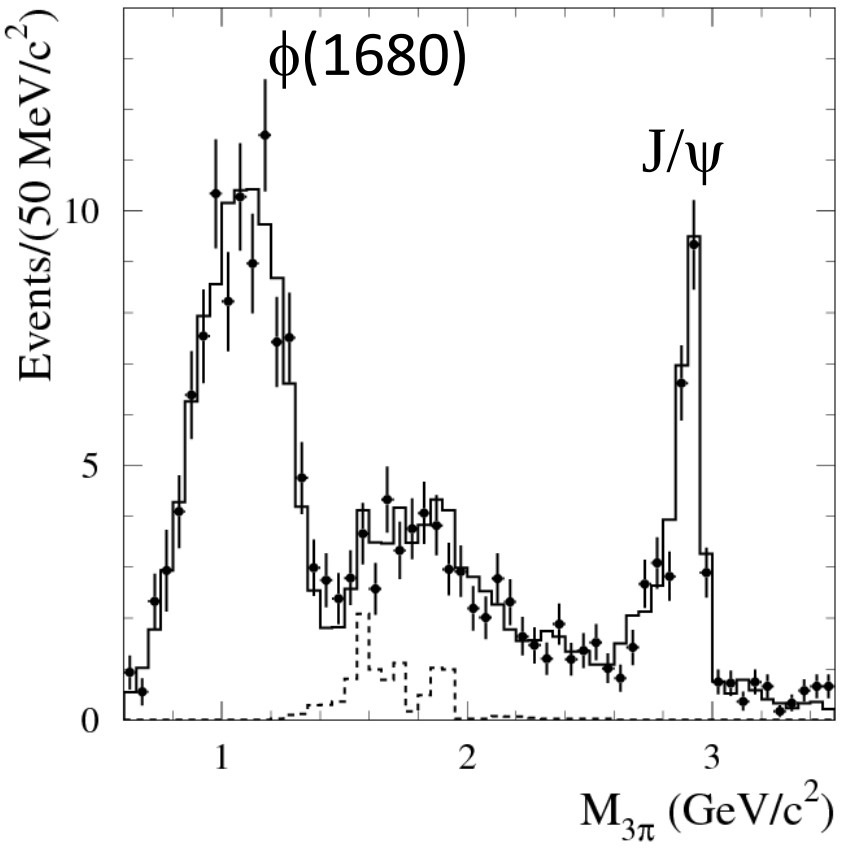

- The mass distribution for background events with charged kaons is obtained from the distribution of events with two identified kaons: $N_{0K} = R_K N_{2K}$.
- The coefficient R_K is determined using MC simulation and corrected to take into account data-MC difference in the kaon identification (in)efficiency. $R_K=(0.12-0.08)\pm0.01$
- The mass distribution obtained is consistent with the mass distribution for simulated $e^+e^- \to K^+K^-\pi^0\gamma$ events.

Background normalization, $e^+e^- \to \pi^+\pi^-\gamma$

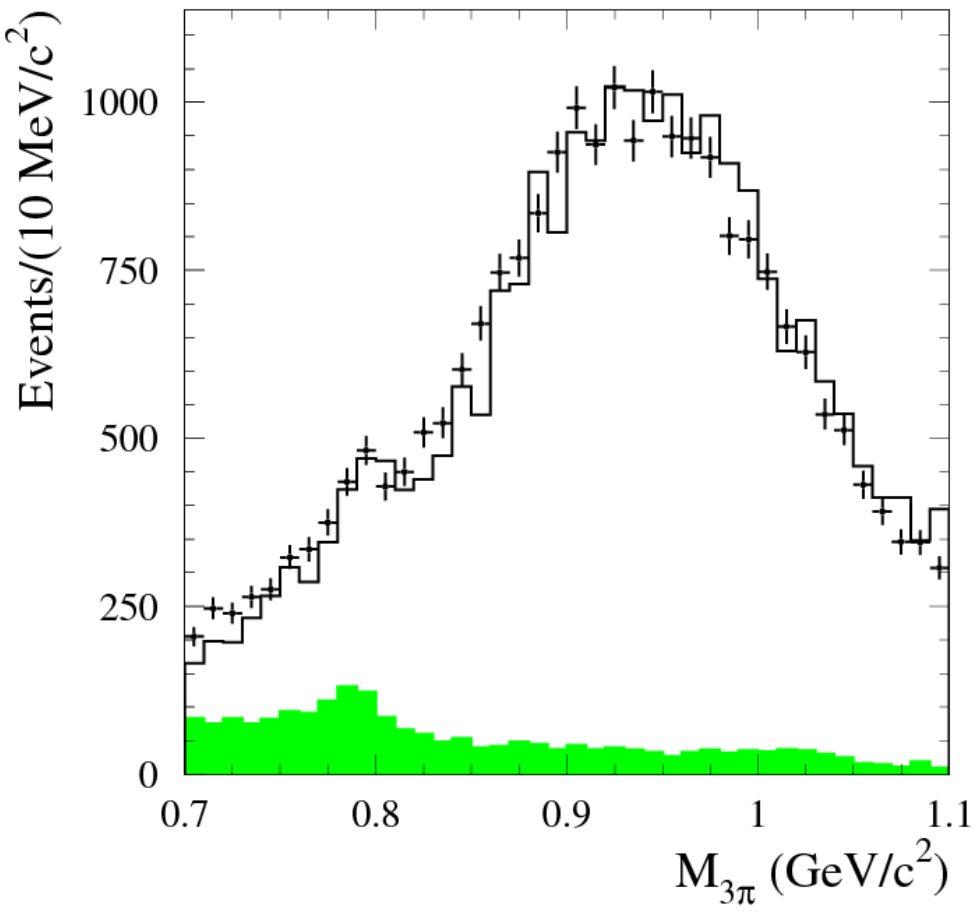

- Events with $40 < \chi^2 < 250$ and $M^2_{rec} < 10$ GeV^2 are used to normalize $\pi^+\pi^-\gamma$ events. M_{rec} is the mass recoiling against $\pi^+\pi^-$ pair.
- The scale factor after the luminosity normalization is 1.60 ± 0.2.
- The large deviation of the scale factor from unity may be due to inaccurate simulation of nuclear interaction of charged π mesons in the calorimeter.

Background normalization, $e^+e^- \to \pi^+\pi^-\pi^0\pi^0\gamma$

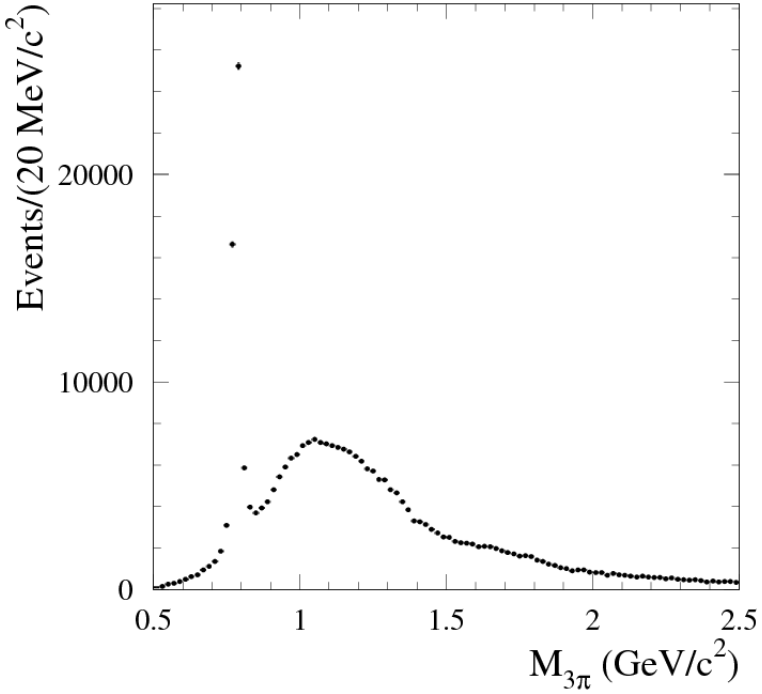

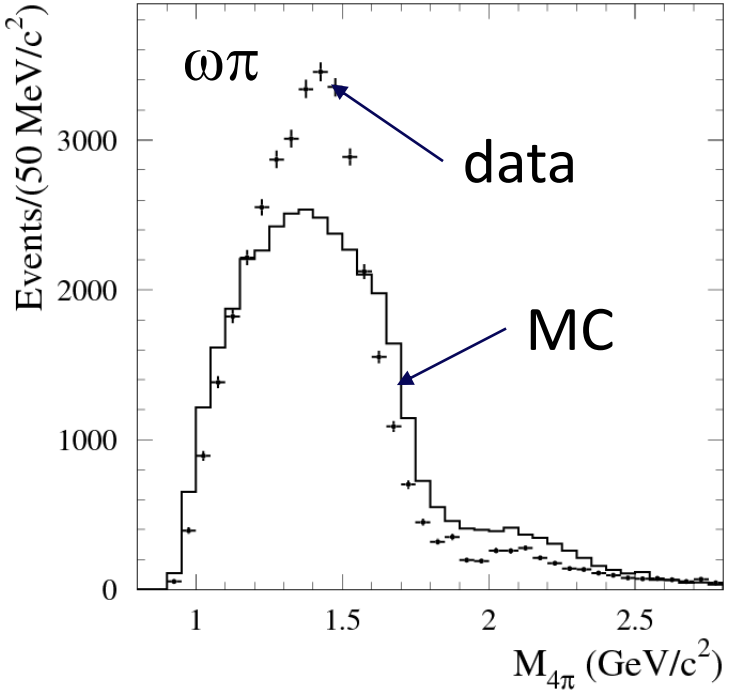

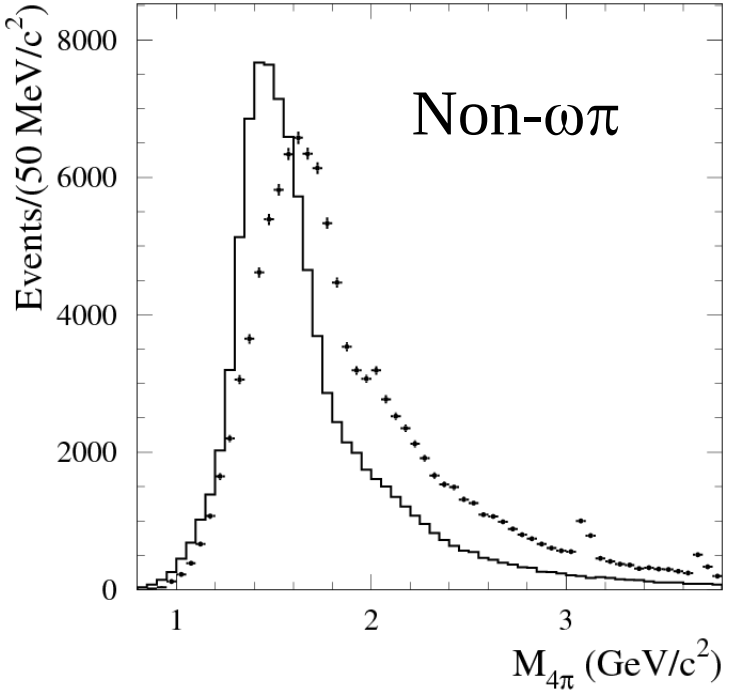

At first stage we select $4\pi\gamma$ events using the kinematic fit to the $e^+e^- \to \pi^+\pi^-\pi^0\pi^0\gamma$ hypothesis and reweight MC events, separately for $\omega\pi$ and non-$\omega\pi$ classes, to reproduce the 4π mass spectra observed in data.

Background normalization, $e^+e^- \to \pi^+\pi^-\pi^0\pi^0\gamma$

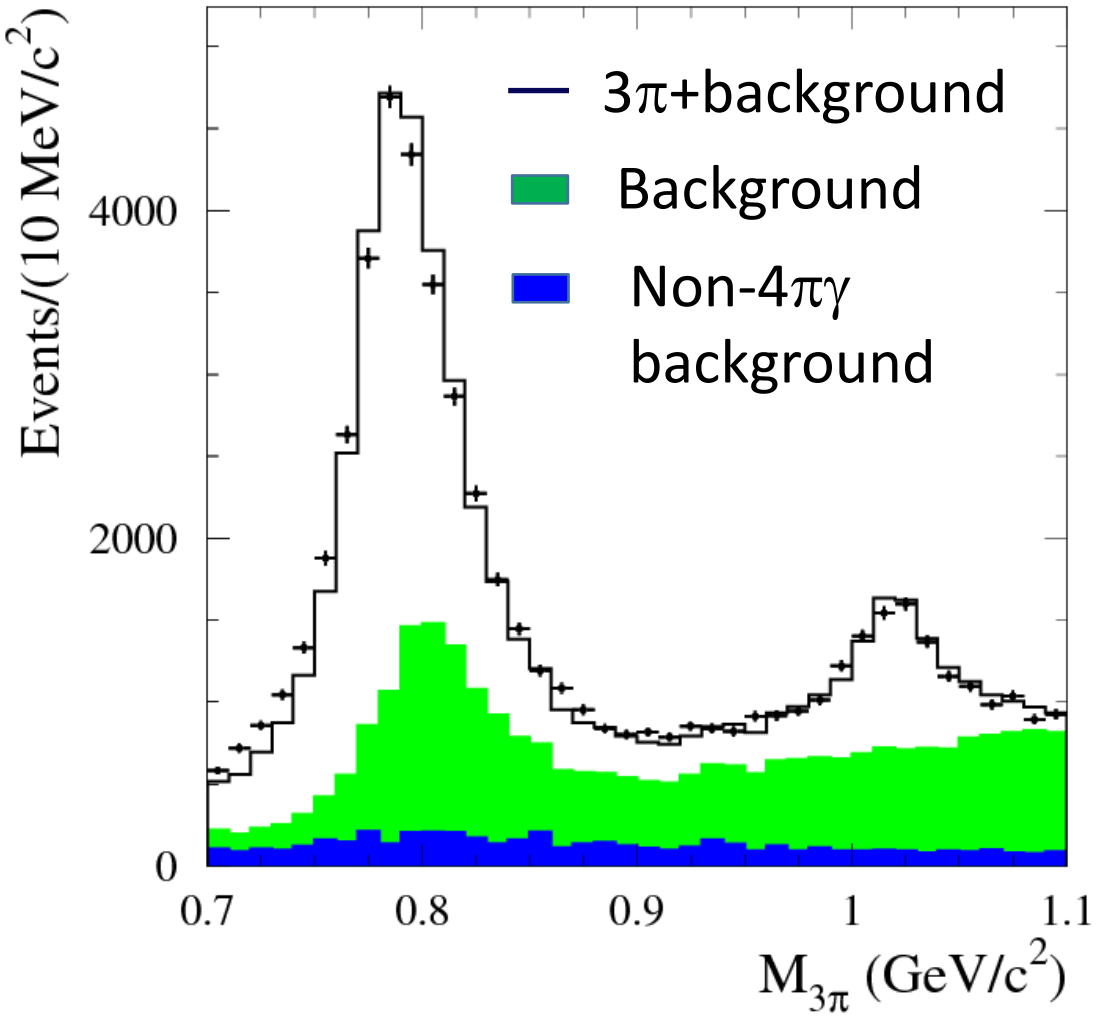

- At the second stage we use 3π candidate events with $50 < \chi^2 < 250$ and $M^2_{rec} > 10$ GeV^2
- The scale factor after the first-step normalization is found to be 1.30 ± 0.15

Background normalization, $e^+e^- \to q\bar{q}$

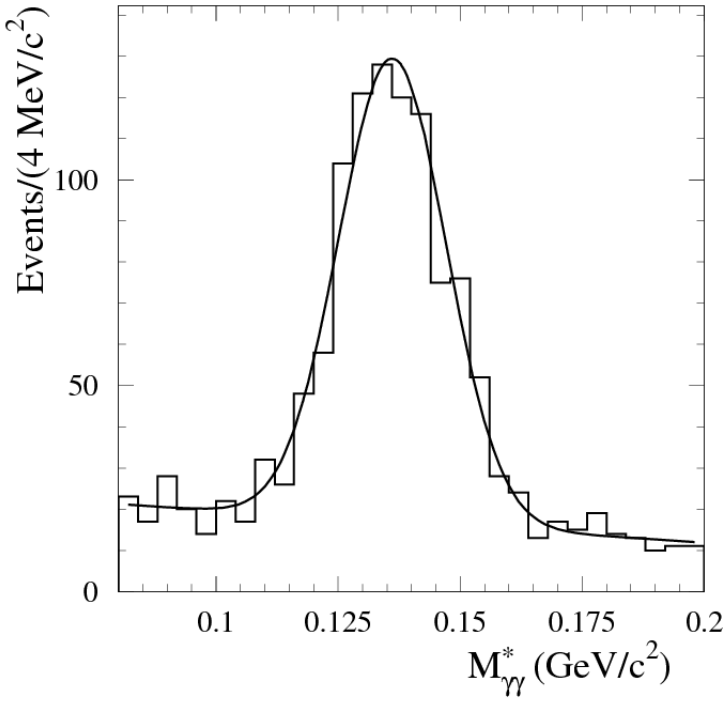

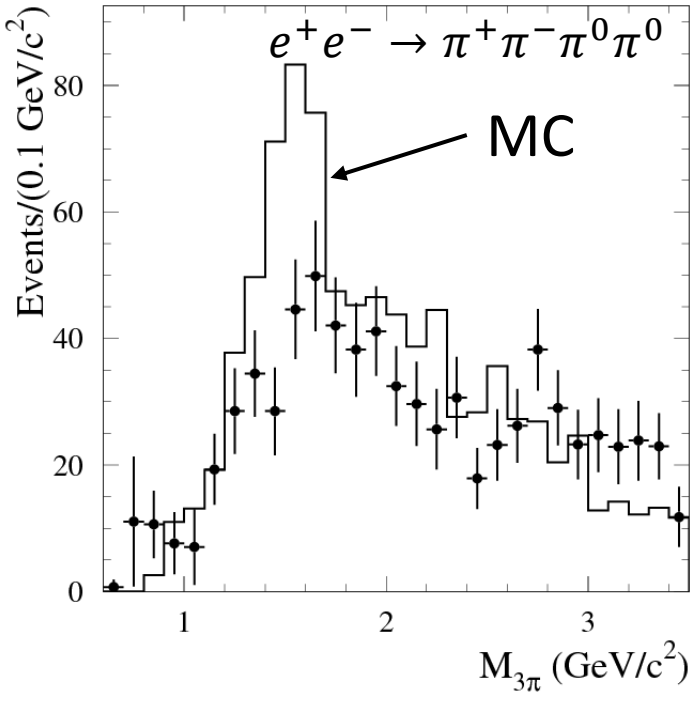

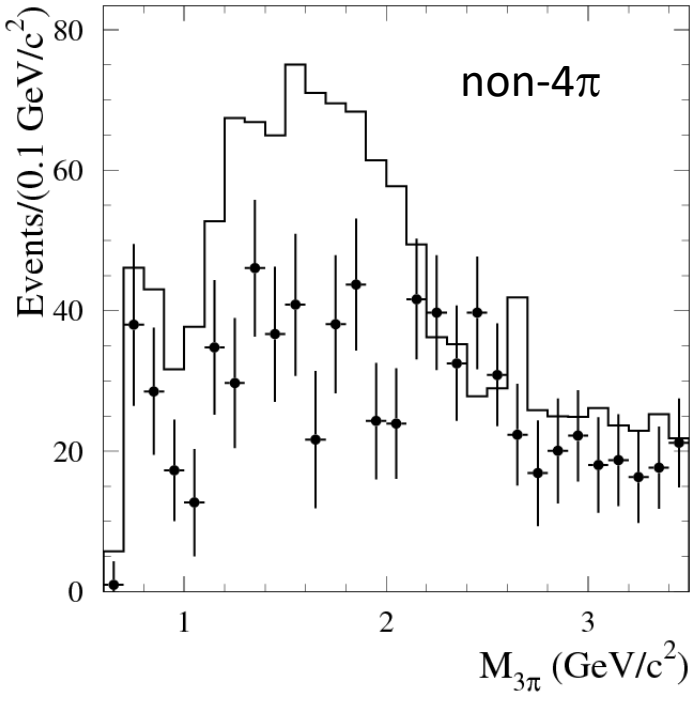

- To estimate $e^+e^- \to q\bar{q}$ background, we analyze the $M^*_{\gamma\gamma}$ spectrum separately for events with $\chi^2 < 40$ (4π) and $40 < \chi^2 < 200$ (non-4π).
- The ratio of data and MC spectra are used to reweight simulation events.

Background normalization, $e^+e^- \to q\bar{q}$

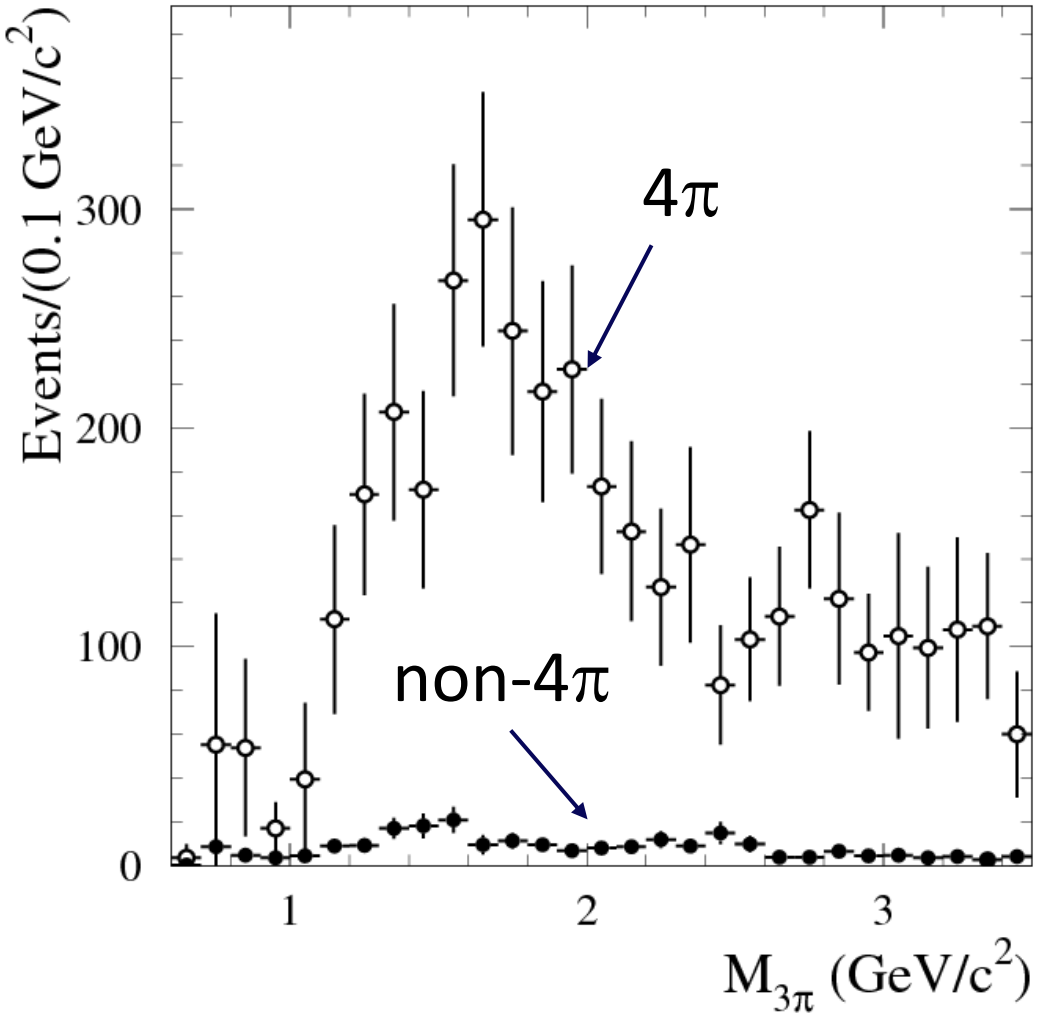

- ✓ The $e^+e^- \to \pi^+\pi^-\pi^0\pi^0$ background has χ^2 distribution close to the distribution for signal events.
- ✓ For the non-4π background we also take into account events containing η meson in the $M^*_{\gamma\gamma}$ spectrum.

Background subtraction, $M_{3\pi} < 1.1$ GeV

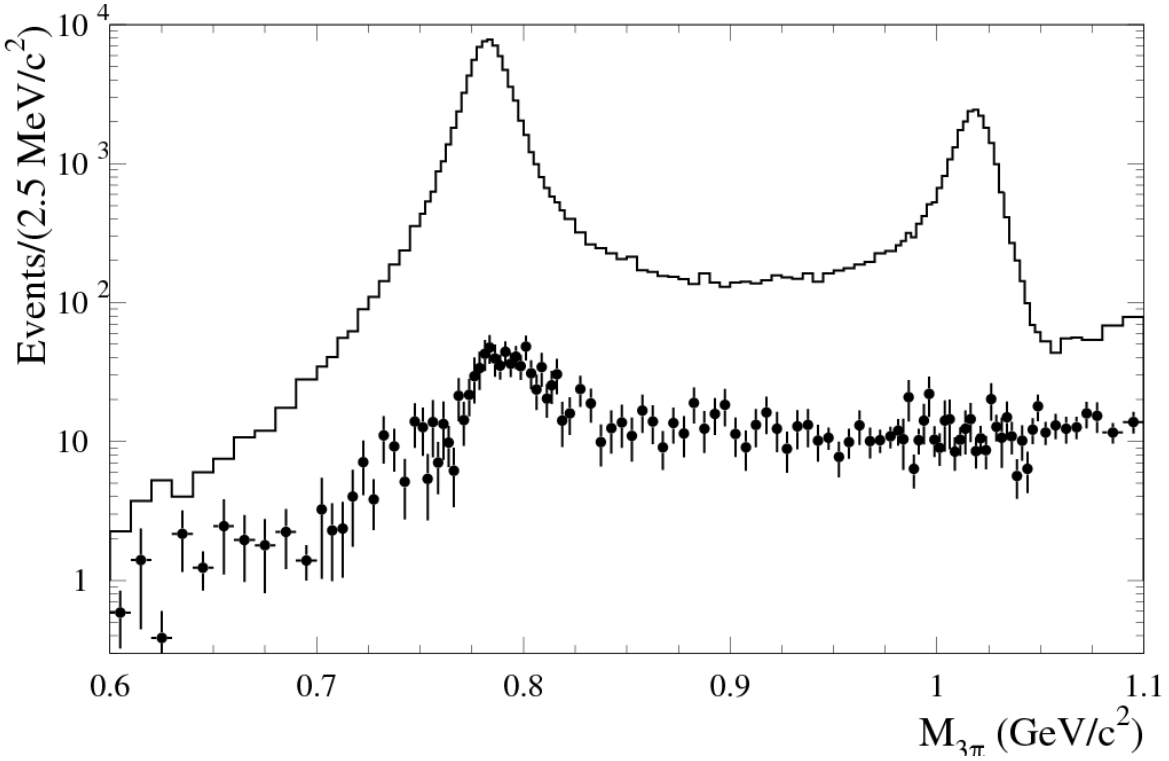

Background spectrum

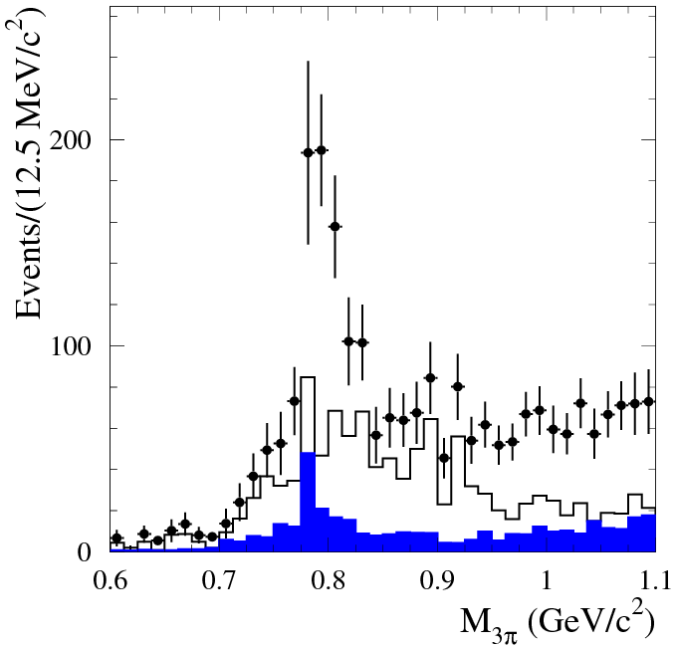

Background fraction

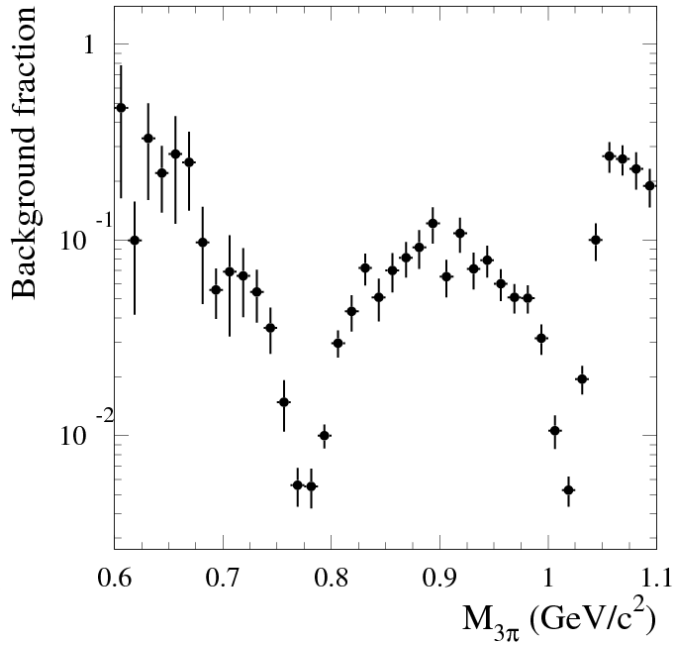

Below 1.1 GeV, where background contribution is relatively small, we subtract estimated background.

Background subtraction, $M_{3\pi} > 1.1$ GeV

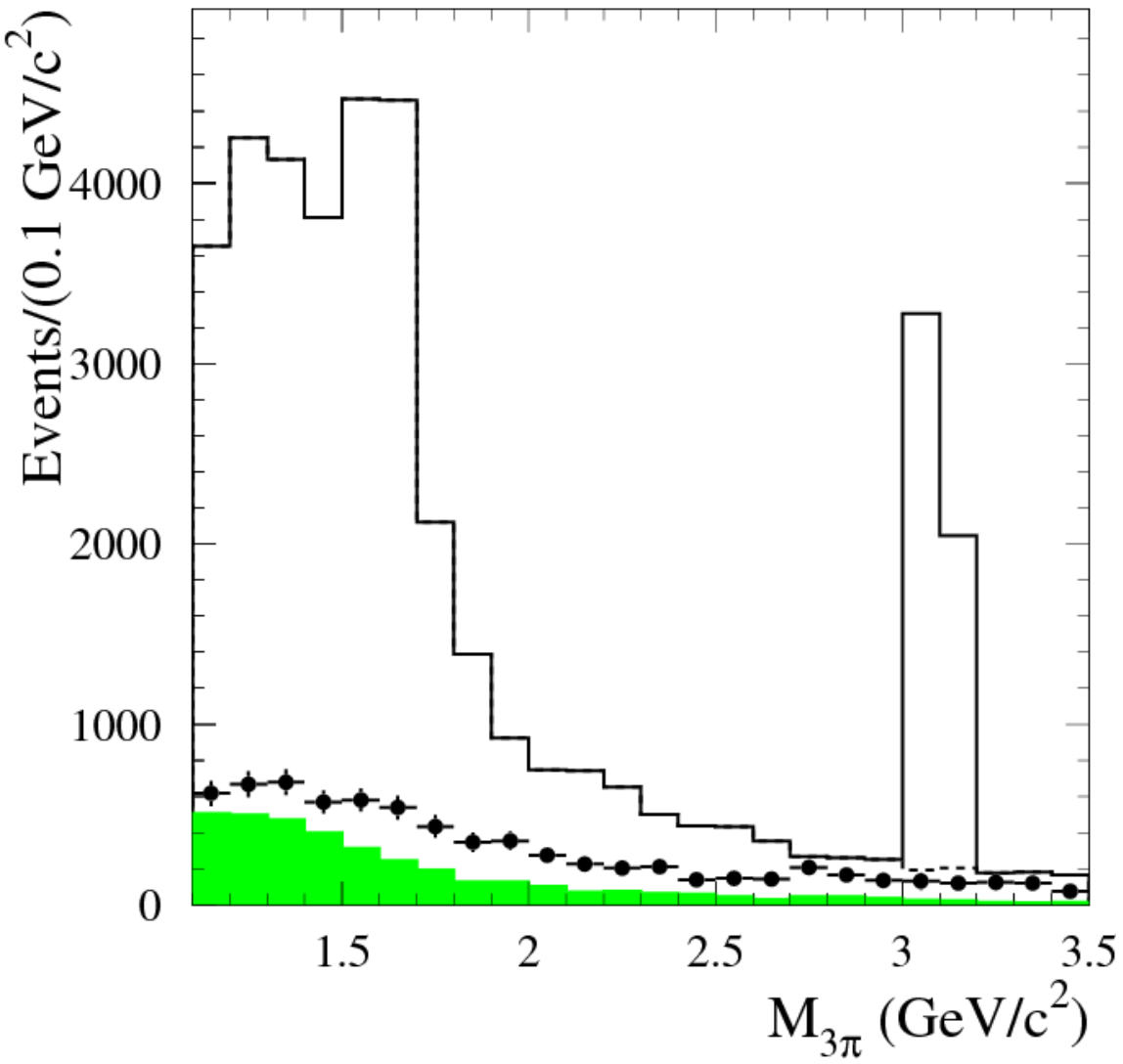

Above 1.1 GeV we use the background subtraction procedure based on difference between signal and background in the χ^2 distribution.

$$N_1' = \alpha_{sig} N_{sig} + \alpha_{bkg} N_{bkg},$$

$$N_2' = (1 - \alpha_{sig}) N_{sig} + (1 - \alpha_{bkg}) N_{bkg}.$$

where N'_1 and N'_2 are the numbers of events with $\chi^2 < 20$ and $20 < \chi^2 < 40$ after subtraction of the 4π and $K^+K^-\pi^0\gamma$ contributions, α_{sig} and α_{bkg} are the N_1/N_2 ratio for signal and background events.

Background subtraction, $M_{3\pi} > 1.1$ GeV

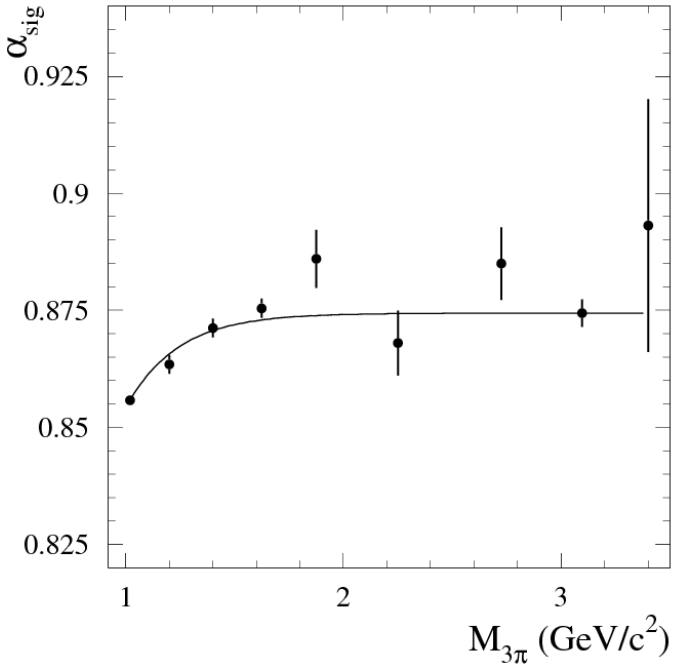

α_{sig} is determined using signal simulation and corrected to data/MC difference. The correction factor is 1.004 ± 0.004 at the ϕ and 1.018 ± 0.007 at the J/ψ. ,α_{bkg} are the N_1/N_2 ratio for signal and background events.

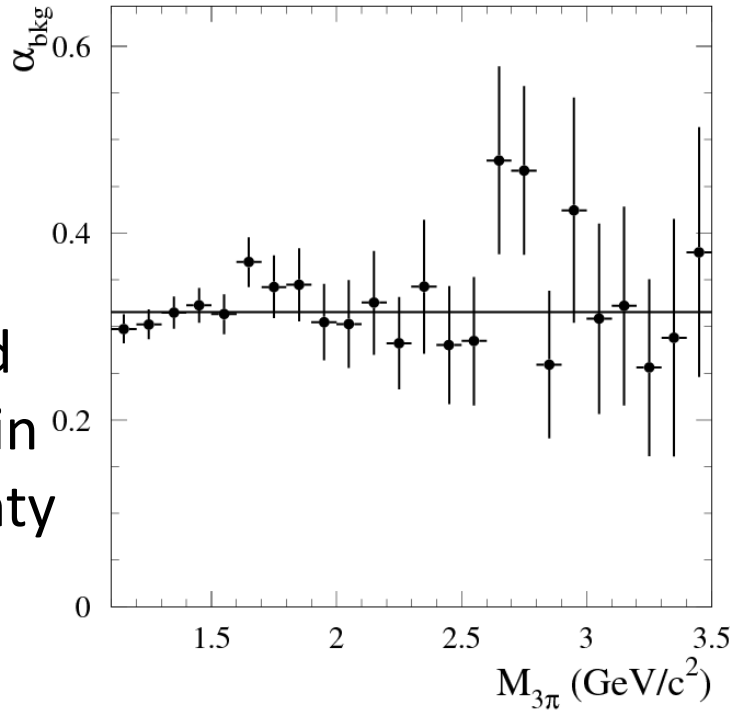

α_{bkg} is is obtained using a mixture of background simulated events. The $e^+e^- \to \pi^+\pi^-\pi^0\pi^0\gamma$ contribution dominates in this mixture. α_{bkg} = 0.316 ± 0.007 with systematic uncertainty of 5% below 2 GeV, 8% between 2 and 3 GeV, and 15% above 3 GeV.

Background subtraction, $M_{3\pi} > 1.1$ GeV

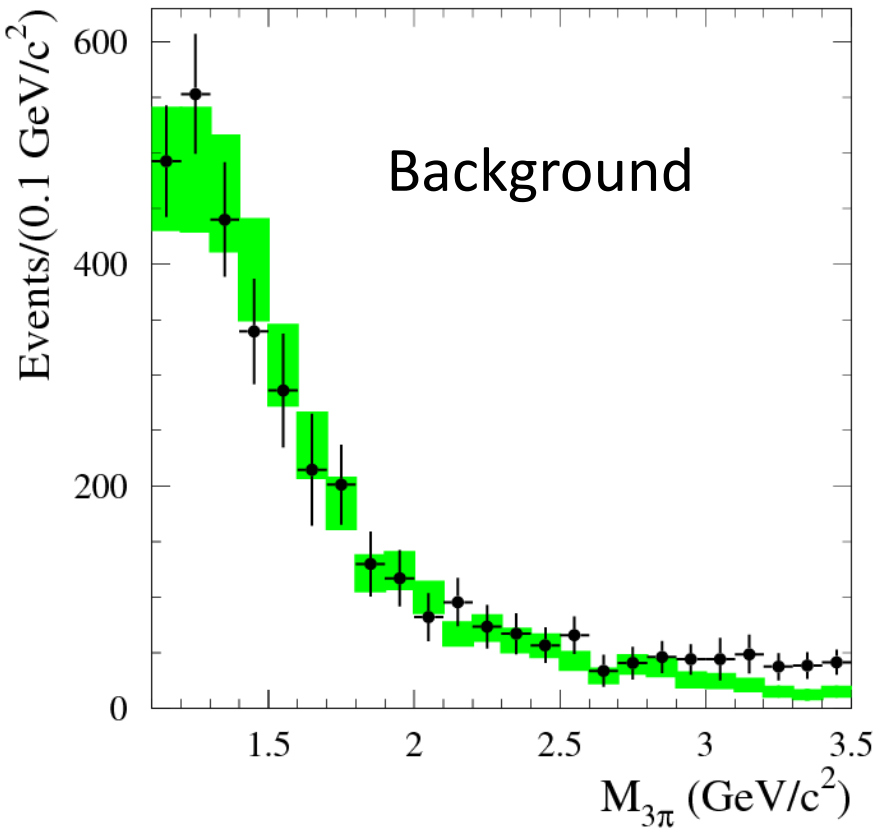

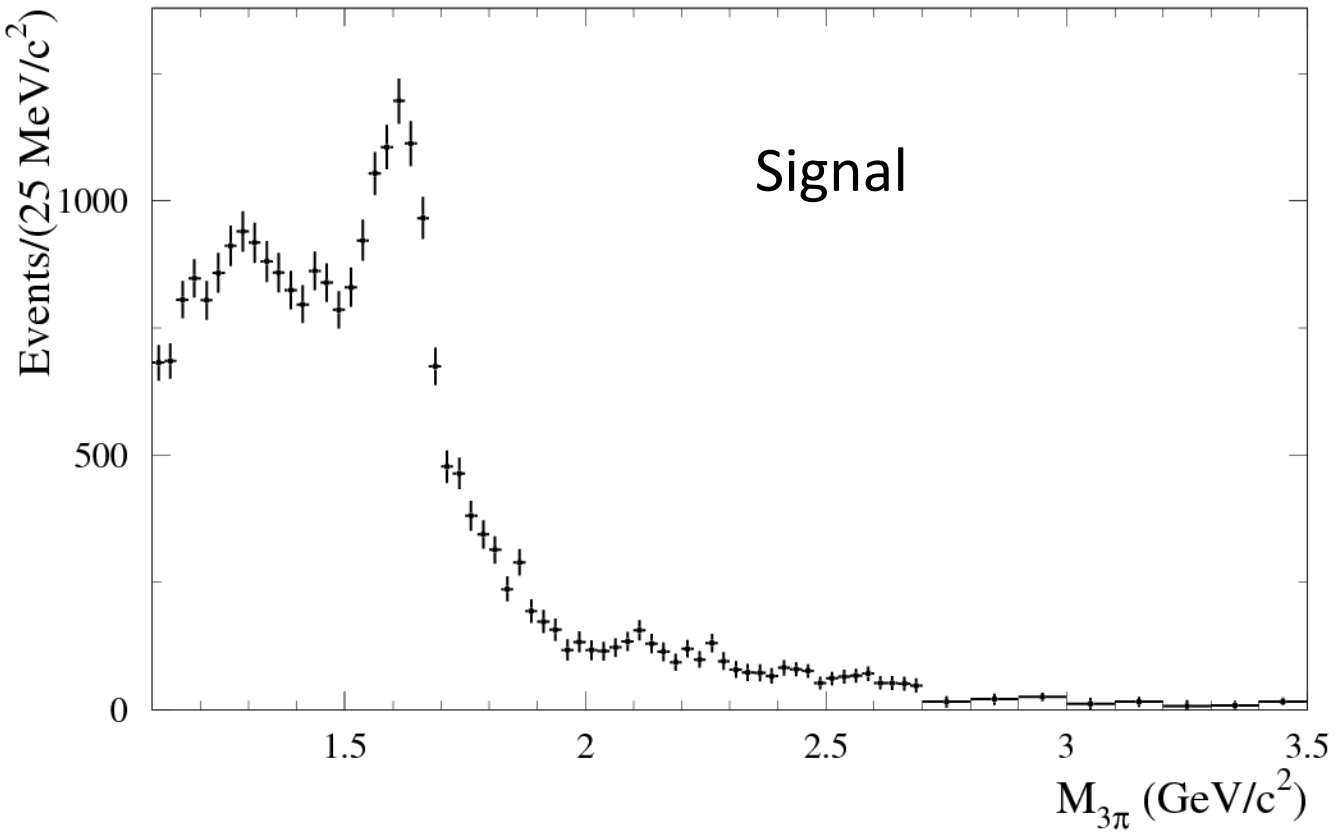

Final state radiation (FSR)

- A high-energy photon can be also emitted from the final state.
- Since the 3π system in the ISR and FSR processes has different C-parity, the interference term vanishes when integrating over the final hadron momenta.
- We analyze two FSR mechanism:

  1. Radiation from charged pions: $\sigma=\sigma(e^+e^-\to 3\pi)f_{FSR}$

  The $e^+e^- \to \pi^+\pi^-\pi^0$ cross section at 10.58 GeV is to be about 4 fb. The probability of photon emission with $E_{\gamma,cm}$>4.7 GeV is $f_{FSR} \approx 0.1(\alpha/\pi)$. So, this FSR mechanism gives a cross section of 0.001 fb and is negligible.

  2. Photon emission from the quarks, which then hadronized into $\pi^+\pi^-\pi^0$. In the 3π mass region under study this process is expected to be dominated by production of resonances decaying to $\pi^+\pi^-\pi^0$, e.g., the processes $e^+e^- \to \eta\gamma$, $a_1(1260)\gamma$, $a_2(1320)\gamma$, ….

Final state radiation (FSR)

The cross sections for the processes $e^+e^- \to a_1(1260)\gamma$ and $a_2(1320)\gamma$ estimated using pQCD are 6.4 fb and 5.4 fb, respectively. The same estimation for the $e^+e^- \to f_2(1260)\gamma$ cross section is 15 fb and in reasonable agreement with BABAR measurement (37^{+24}_{-18}) fb.

The next group of C-even resonances decaying to $\pi^+\pi^-\pi^0$ is located near 1.7 GeV: $a_1(1640)$ and $a_2(1700)$. Their cross sections are estimated to be about 2 times lower than those for a_1 and a_2.

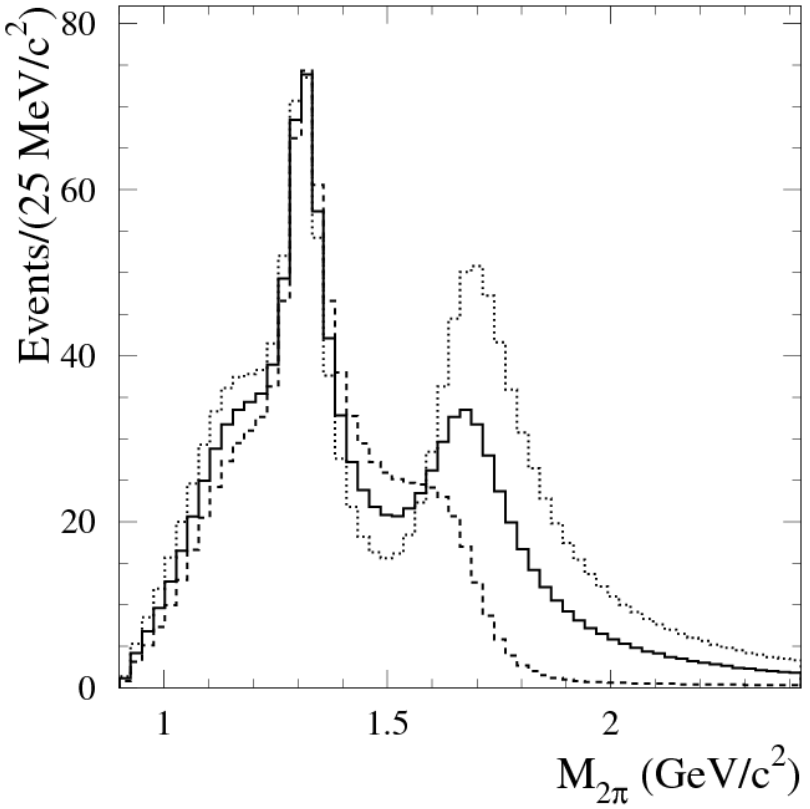

Interference between amplitudes of different resonances may strongly modify the spectrum. We subtract the spectrum without interference from the spectra for selected data events. The systematic uncertainty is taken to be 100%.

The fraction of the FSR background is 7–8% in the region 1.05–1.08 GeV and near 1.32 GeV. Near 1.7 GeV the background fraction is about 6%.

Detection efficiency

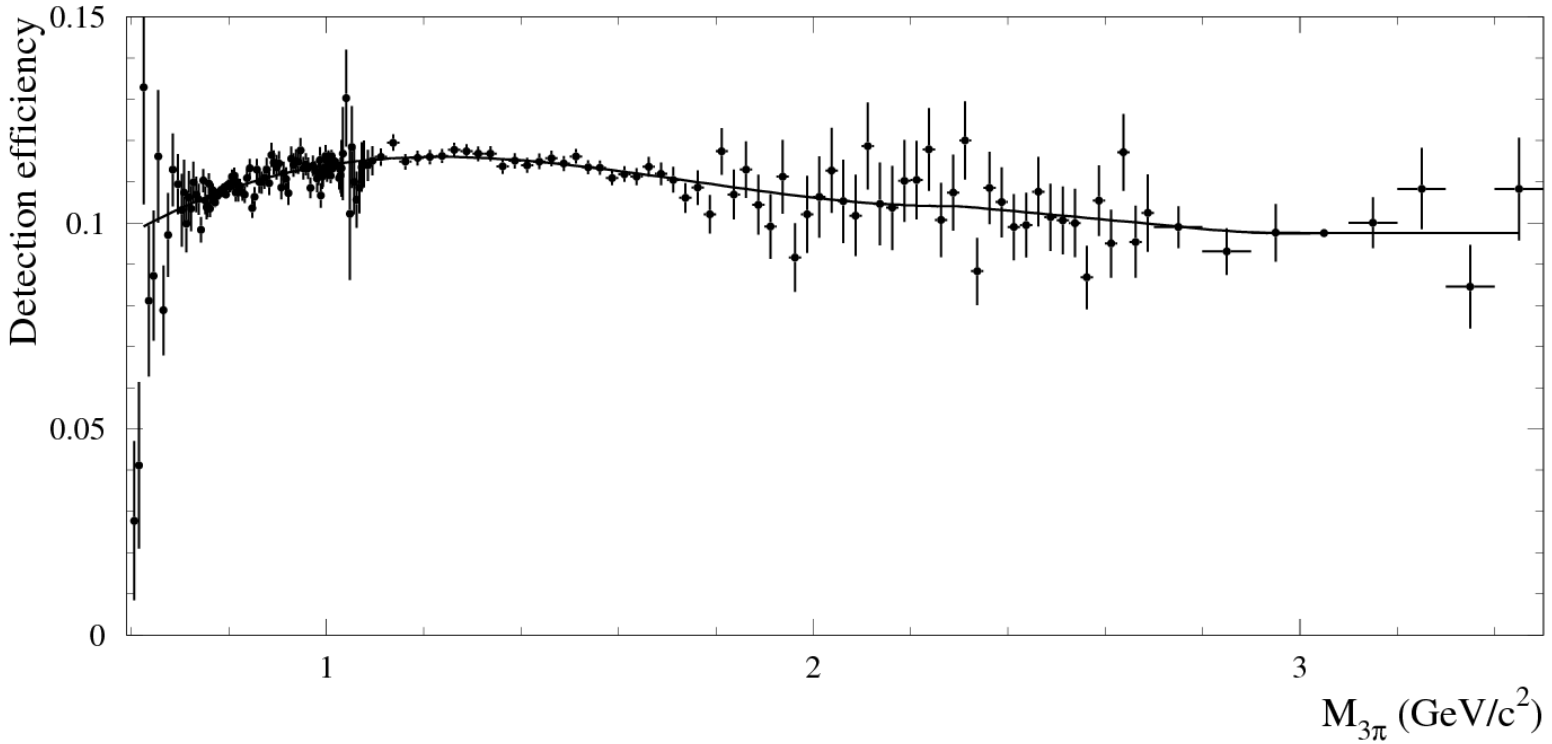

The detection efficiency obtained using simulation is corrected to take into account data-MC difference in detector response

$$\varepsilon = \varepsilon_{MC} \Pi (1 + \delta_i)$$

Efficiency corrections

The efficiency corrections are estimated using

- ✓ $e^+e^- \to \mu^+\mu^-\gamma$ events (ISR photon detection efficiency, data-MC difference in the χ^2 distribution)
- ✓ $3\pi\gamma$ events at ω, ϕ, and J/ψ (π^0 loss, background suppression cuts)
- ✓ prescaled events (radiative Bhabha suppression, filter inefficiency)

π^0 reconstruction inefficiency

To study the π^0 losses, we perform a kinematic fit to the $e^+e^- \to \pi^+\pi^-\pi^0\gamma$ hypothesis using the measured parameters for only the two charged tracks and the ISR photon. The π^0 energy and angles are determined as a result of the fit.

Then we determine the numbers of events under the ω peak for events with $\chi^2 < 40$ and $\chi^2 > 40$ in data and simulation.

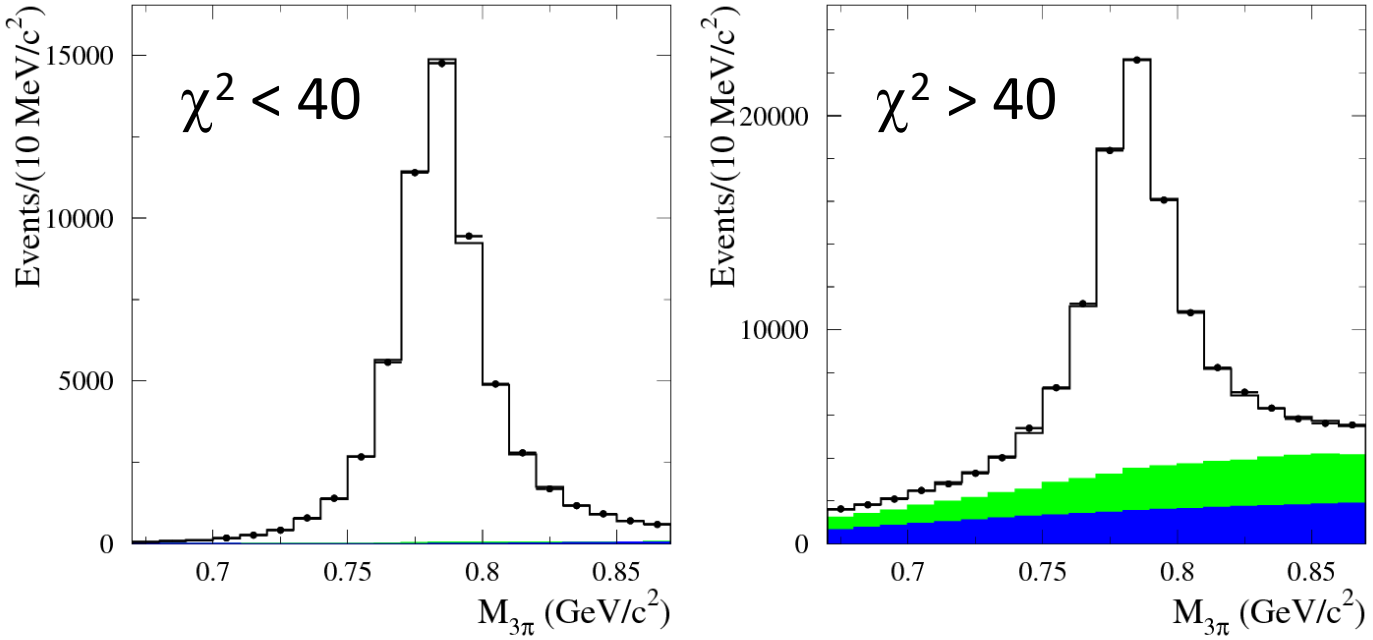

The data/MC difference in the π^0 reconstruction inefficiency is independent of π^0 energy and is found to be $-(3.4 \pm 0.5)\%$.

Data-MC difference in the χ^2 distribution.

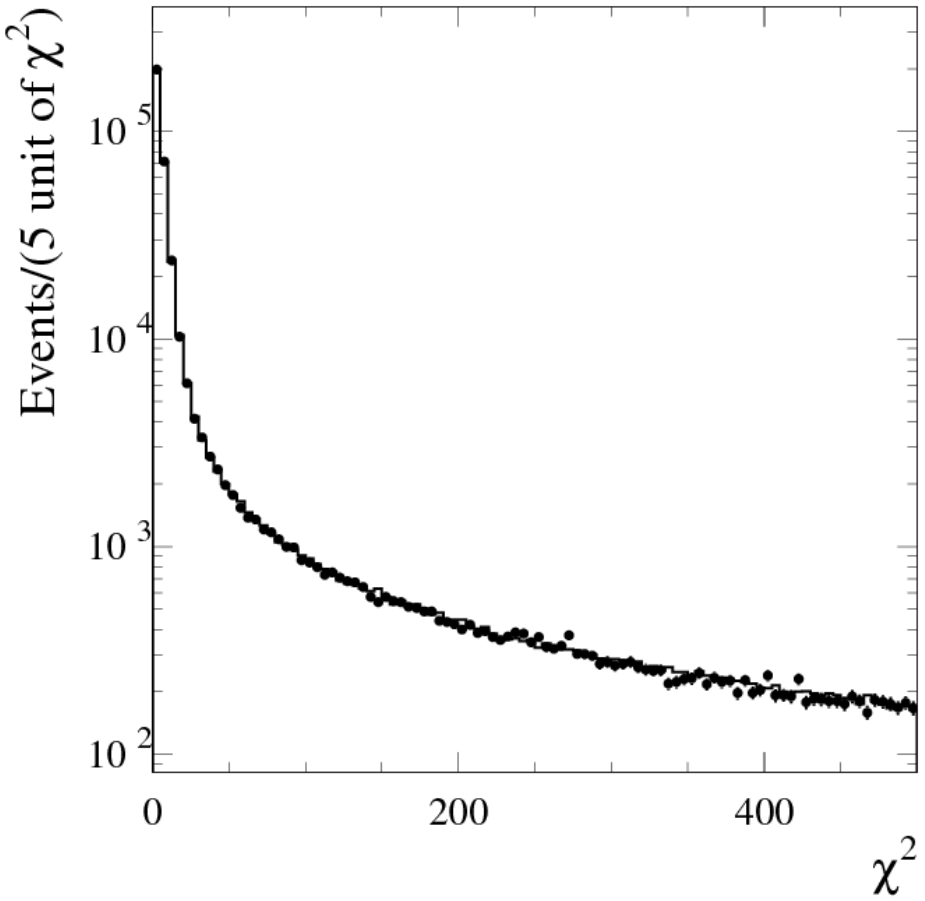

- The π^0 correction includes a part of the efficiency correction due to the $\chi^2 < 40$ cut related to the photons from the π^0 decay.
- To understand influence of the data-simulation difference in the parameters of the charged tracks and the ISR photon, we study $e^+e^- \rightarrow \mu^+\mu^-\gamma$ events.
- The correction is found to be $-(0.4\pm0.2)\%$ in the 3π mass region below 1.1 GeV and $-(1 \pm 1)\%$ above.

Efficiency correction due to track losses

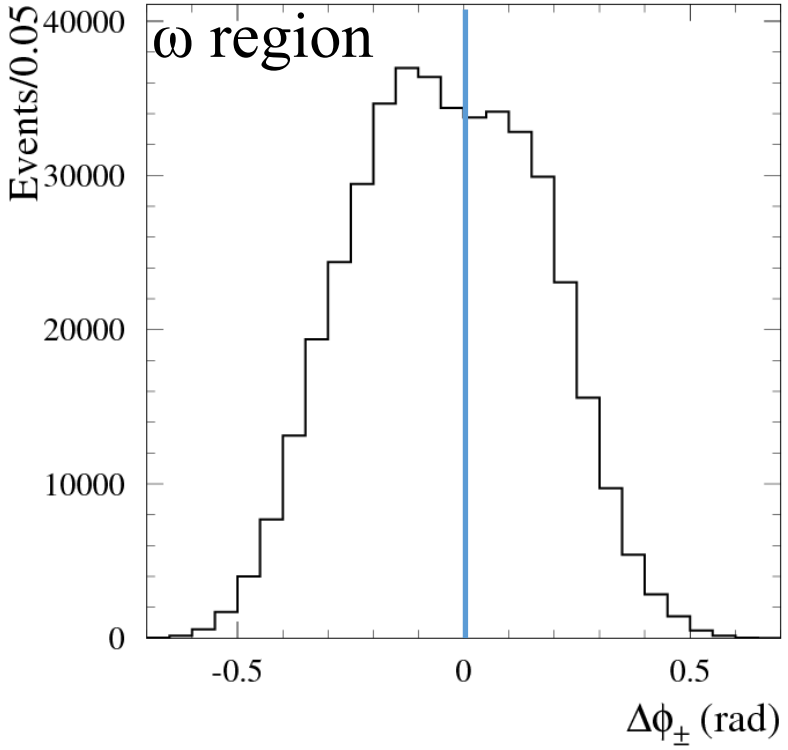

$$f_{\text{overlap}} = \frac{N(\Delta\varphi_{\pm} < 0) - N(\Delta\varphi_{\pm} > 0)}{2N(\Delta\varphi_{\pm} < 0)}$$

- To study the data-MC simulation difference in track losses for isolated tracks is studied using $e^+e^- \rightarrow \tau^+\tau^-$ events. No difference between data and simulation is observed within an uncertainty of 0.24% per track.
- To study the effect of track overlap we analyze the distribution of the azimuthal angle difference between the positive and negative tracks.
- Events with $\Delta\varphi_{\pm} > 0$ exhibit a "fishtail" two-track configuration in which the tracks tend to overlap.
- The fraction of events lost because of track overlap is 11% at the ω, 8% at the ϕ, and about 1% at the J/ψ.
- However, the data-MC difference is −(0.03±0.23)% below 1.1 GeV.

Efficiency corrections

TABLE I. Efficiency corrections (in %) for different effects in three $M_{3\pi}$ regions.

effect	$M_{3\pi} < 1.1$ GeV/c^2	$1.1 < M_{3\pi} < 2$ GeV/c^2	$M_{3\pi} > 2$ GeV/c^2
photon efficiency	-1.0 ± 0.2	-1.2 ± 0.2	-1.4 ± 0.2
π^0 loss	-3.4 ± 0.5	-3.4 ± 0.5	-3.4 ± 0.5
$\chi^2_{3\pi\gamma}$ distribution	-0.4 ± 0.4	-1 ± 1	-1 ± 1
rad. Bhabha suppression	0.0 ± 0.1	0.0 ± 0.1	0.0 ± 0.1
background suppression	0.4 ± 0.2	0.6 ± 0.5	0.6 ± 0.8
track loss	0.0 ± 0.5	0.0 ± 0.5	0.0 ± 0.5
trigger and filters	-1.4 ± 0.7	-1 ± 1	-1 ± 1
total	-5.8 ± 1.1	-6.0 ± 1.7	-6.2 ± 1.8
$\chi^2_{3\pi\gamma} < 20$	0.1 ± 0.1 at ω 0.4 ± 0.4 at ϕ	0.5–1.1	1.1–1.8

Model uncertainty in the detection efficiency

- ✓ The $\rho(770)\pi$ model used in signal simulation works well in the ω and ϕ mass region, below 1.1 GeV.
- ✓ SND@VEPP-2000 performed a Dalitz plot analysis in the energy range 1.05-2 GeV and observed a significant contribution of the $\rho(1450)\pi$ mechanism near the $\omega(1650)$.
- ✓ The contribution of the $\omega\pi^0$ mechanism and its interference with the $\rho\pi$ amplitude reaches 20% of the total cross section at 1.3 GeV.

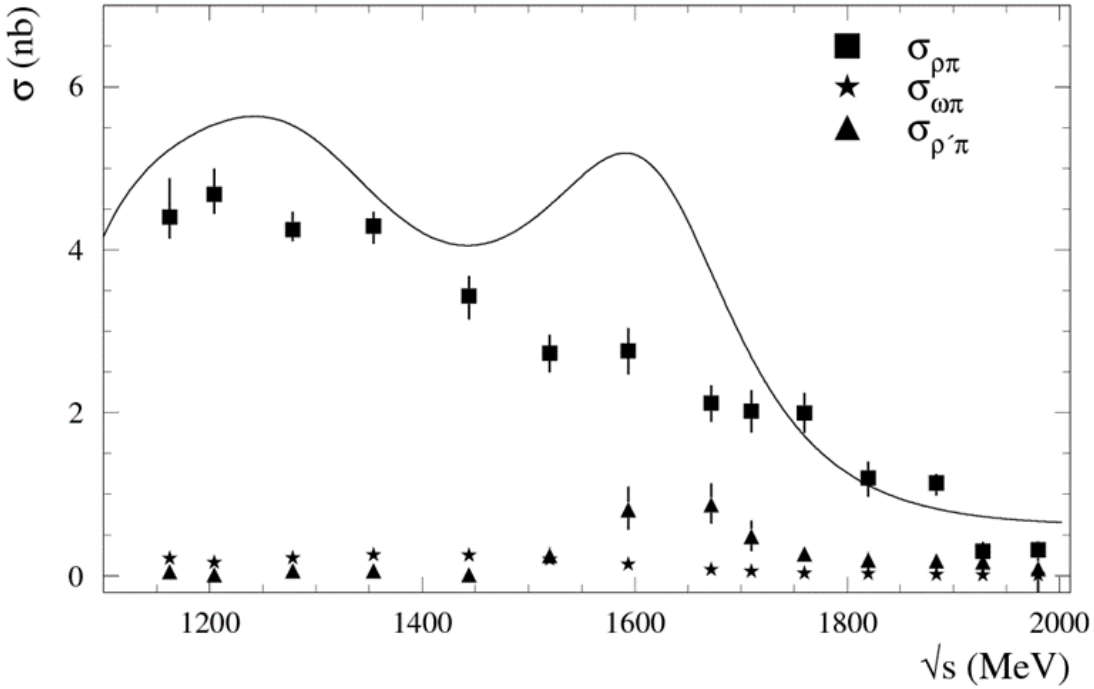

- ❑ We reweight simulated events using the model with a sum of the $\rho(770)\pi$, $\omega\pi^0$, and $\rho(1450)\pi$ mechanisms with coefficients and relative phases taken from the SND measurement.
- ❑ The difference in the detection efficiency between the two models depends on energy but does not exceed 1.5%. This number is taken as an estimate of the model uncertainty of the detection efficiency above 1.1 GeV.

Strategy of cross-section measurement

- Below 1.1 GeV, where the narrow ω and ϕ resonances dominate in the 3π cross section, we perform unfolding of the resolution and FSR effects from the measured 3π mass spectrum.
- Above 1.1 GeV, where resonances are wide, and the finite mass resolution does not distort significantly the mass spectrum, the measured spectrum is used to obtain the 3π cross section.

$\pi^+\pi^-\pi^0$ mass spectrum below 1.1 GeV

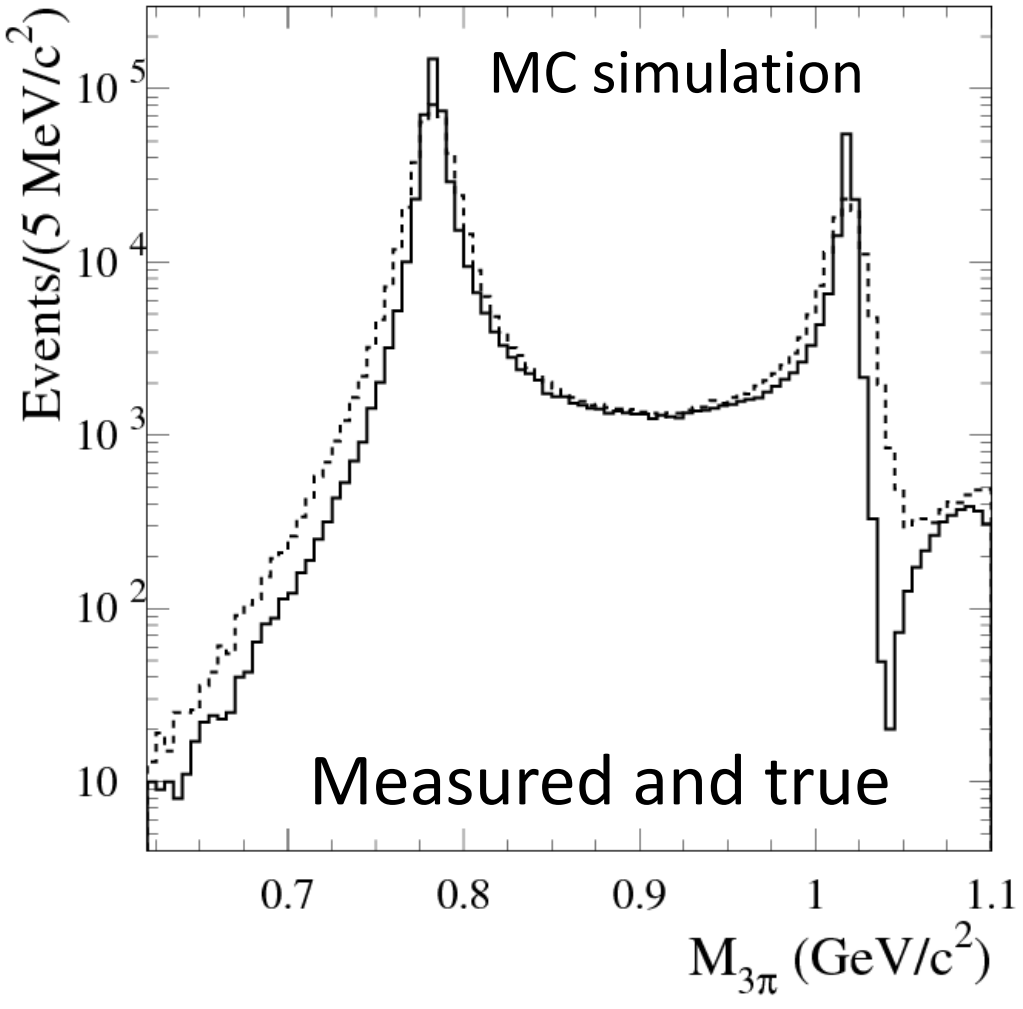

- The mass spectrum varies by 5 orders of magnitude and has narrow peaks. The result of unfolding strongly depends on quality of mass-resolution simulation.
- To study data-MC difference in resolution, we fit to the observed mass spectrum with the VMD model.
- The widths of the ω and ϕ resonances are measured with high accuracy. From the fit we determine parameters of the (narrow) Gaussian smearing function.
- The long tails of the mass resolution function depend on requirement on χ^2 of the kinematic fit used for event selection. To understand quality of the tail simulation, we compare results of the VMD fit for spectra obtained with different cuts on χ^2.

Fit to the 3π mass spectrum

- The measured mass spectrum is fitted by the VMD model with ω(782)+ρ(770)+ϕ(1020)+ω(1420)+ω(1680)
- The true spectrum is smeared to take into account data-MC difference in the resolution and then multiplied by the transfer matrix obtained using simulation

$$\left(\frac{dN}{dm}\right)_i^{meas} = (1-\epsilon)\sum_j P_{ij}\left[\left(\frac{dN}{dm}\right) * G\right]_j + \epsilon\left[\left(\frac{dN}{dm}\right) * L\right]_i$$

- The Gaussian describes broadening of the ω and ϕ peaks, while the Lorentzian (Breit-Wigner) describes the data-MC difference in the tails of the resolution function.
- The branching fraction for the ρ→3π decay is expected to be about 10^{-4}. The only SND measurement is $(1.01^{+0.54}_{-0.36} \pm 0.34) \times 10^{-4}$

Fit to the 3π mass spectrum

Model	Lorentzian smearing	$\mathcal{B}(\rho \to 3\pi)$	χ^2/ν
1	yes	free	136/127
2	no	$\equiv 0$	201/131
3	yes	$\equiv 0$	180/129
4	no	free	147/129

- It is seen that the data spectrum cannot be described with zero branching fraction for the ρ→3π decay.
- The smearing Gaussian sigma is found to be 1.5±0.2 MeV.
- The significance for the Lorentzian smearing is about 3σ.

Fit to the 3π mass spectrum (models 1-3)

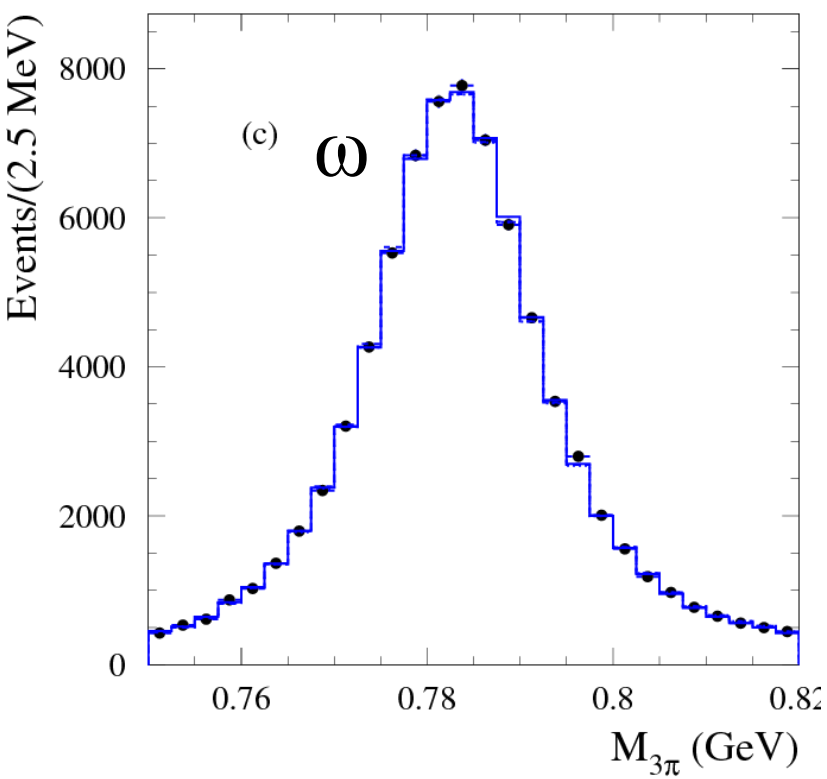

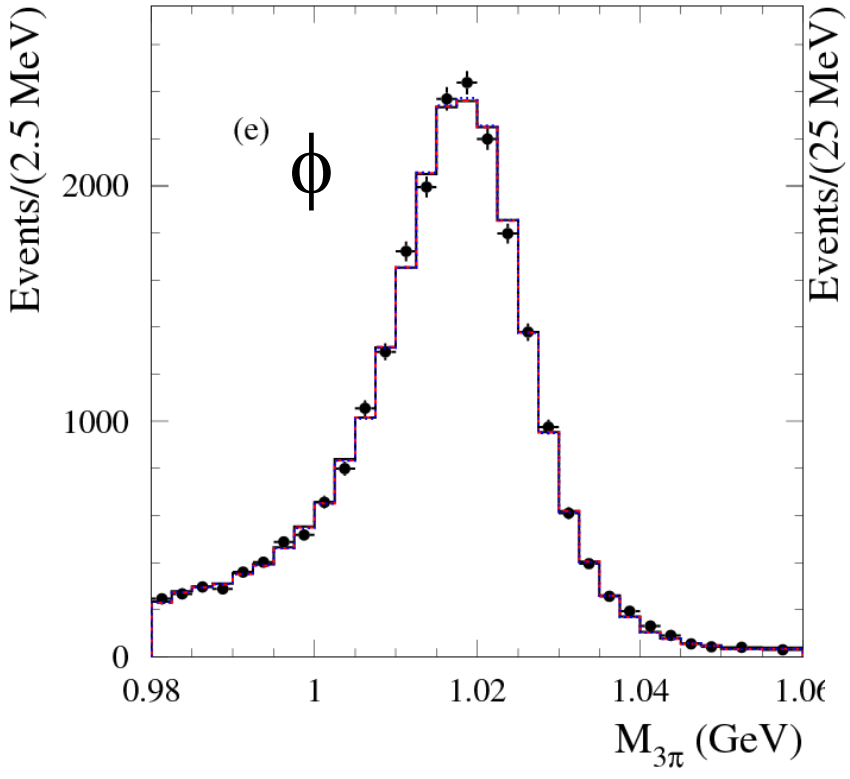

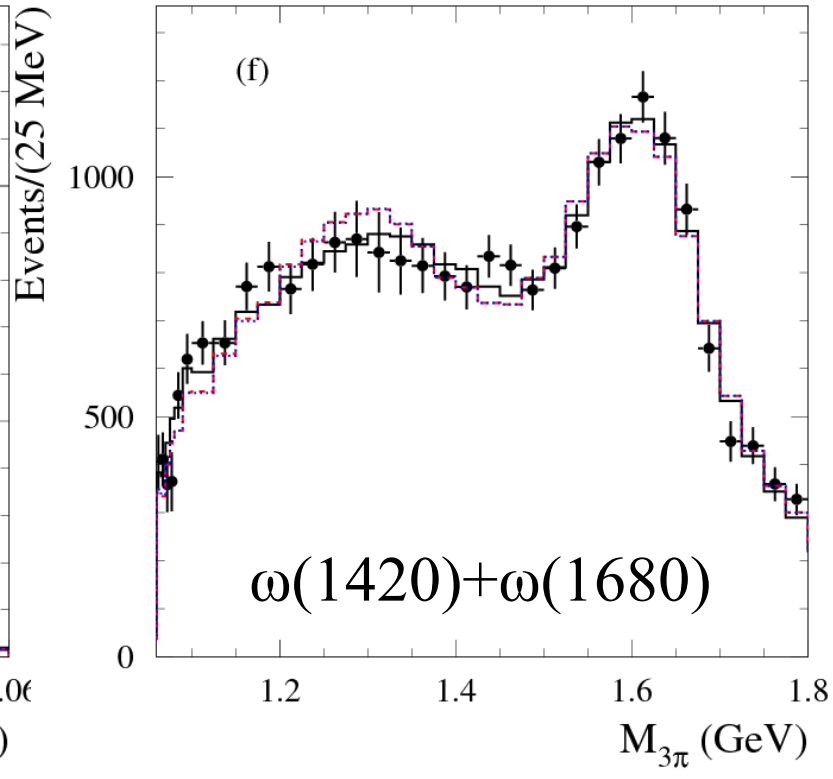

- ✓ In the ω and ϕ regions and all three models give the same result.
- ✓ Above 1.1 GeV the models with $B(\rho \to 3\pi)=0$ describe data worse.

Fit to the 3π mass spectrum (models 1-3)

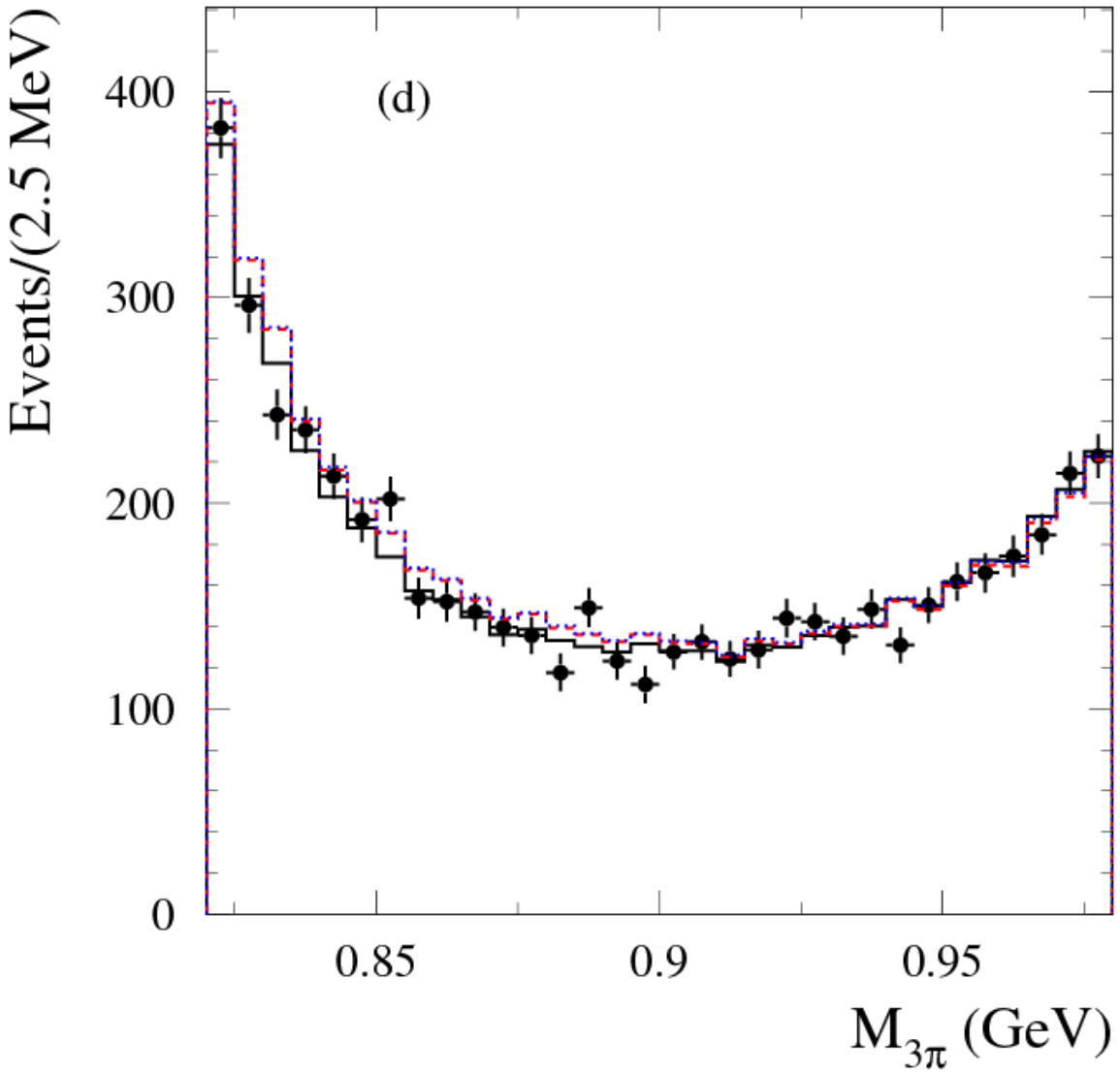

Data between ω and ϕ cannot be described by the models with $B(\rho \rightarrow 3\pi)=0$

Fit to the 3π mass spectrum (models 1 и 4)

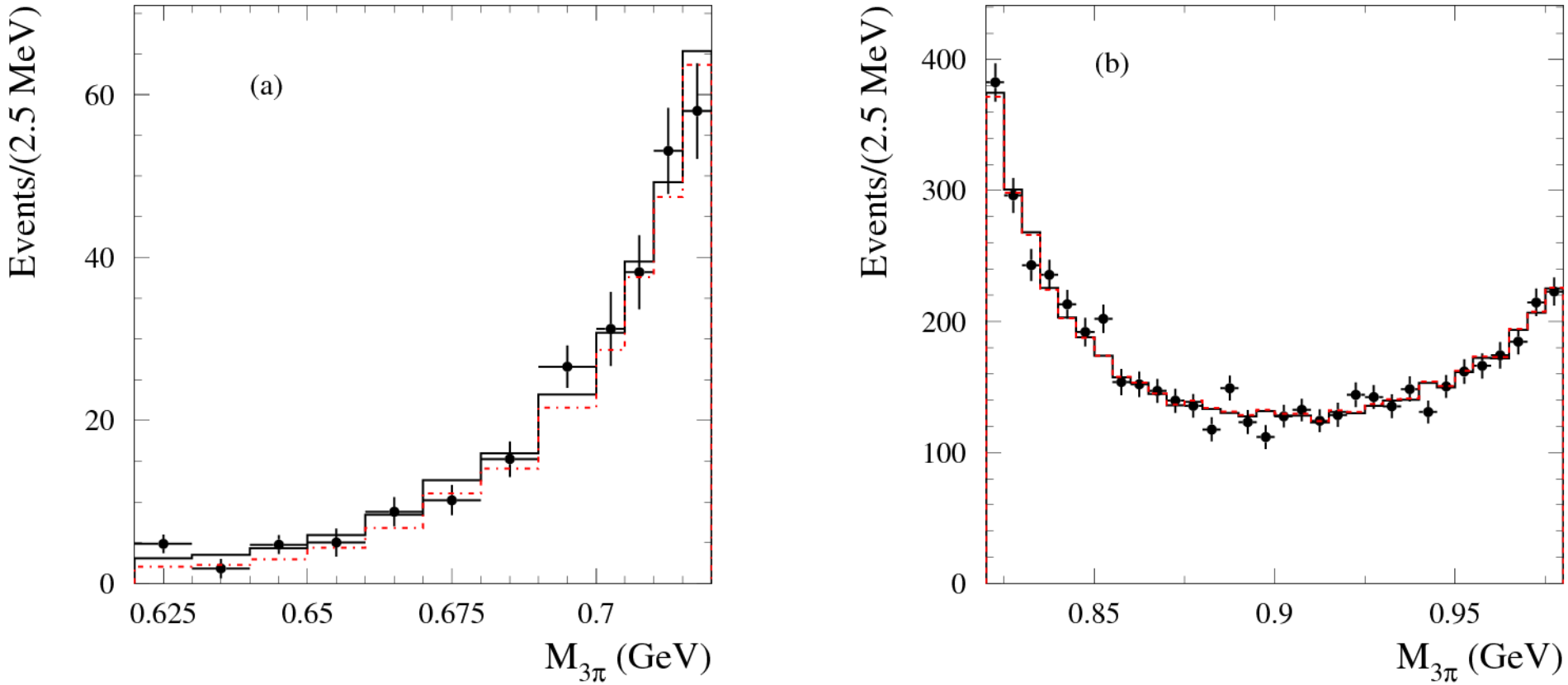

- ✓ The difference between Model 1 and Model 4 (free B(ρ → 3π), no Lorentzian smearing) is maximal in the 3π mass region 0.62–0.72 GeV.
- ✓ The fit with Model 4 increase B(ρ → 3π) by about 20%.

Fit to the 3π mass spectrum, $\chi^2 < 20$

To reduce the influence of the data-simulation difference in resolution to the fitted parameters, we tighten the condition on χ^2 of the kinematic fit from 40 to 20.

Model	BW smearing	$\mathcal{B}(\rho \to 3\pi)$	χ^2/ν
1	yes	free	135/127
2	no	$\equiv 0$	181/131
3	yes	$\equiv 0$	178/129
4	no	free	136/129

- Inclusion of the Lorentzian smearing improves the fit quality insignificantly.
- Therefore, we use the fit model without the Lorentzian smearing.
- σ_s = 1.5±0.2 MeV, $m_\omega - m_{PDG}$ = 0.042±0.055 MeV, $m_\phi - m_{PDG}$ = 0.095 ± 0.084 MeV.

Physical fit parameters

$$\Gamma(\omega \to e^+e^-)\mathcal{B}(\omega \to \pi^+\pi^-\pi^0) = (0.5698 \pm 0.0031 \pm 0.0082)\ \text{keV}$$

$$\Gamma(\phi \to e^+e^-)\mathcal{B}(\phi \to \pi^+\pi^-\pi^0) = (0.1841 \pm 0.0021 \pm 0.0080)\ \text{keV}$$

$$\mathcal{B}(\rho \to 3\pi) = (0.88 \pm 0.23 \pm 0.30) \times 10^{-4}$$

$$\phi_\rho = -(99 \pm 9 \pm 15)^\circ.$$

- The significance of ρ → 3π is greater than 6σ
- The fitted parameters for ω and ϕ are in reasonable agreement with the world average values: 0.557±0.011 keV and 0.1925±0.0043 keV.
- The BABAR results for $B(\rho \to 3\pi)$ and ϕ_ρ agree with the SND measurement: $B(\varrho \to 3\pi) = (1.01^{+0.54}_{-0.36} \pm 0.34) \times 10^{-4}$ and $-(135^{+17}_{-13} \pm 9)^\circ$

TABLE VI: Contributions to the systematic errors of fit parameters from different effects ($P_1 = \Gamma(\omega \to e^+e^-)\mathcal{B}(\omega \to \pi^+\pi^-\pi^0)$, $P_2 = \Gamma(\phi \to e^+e^-)\mathcal{B}(\phi \to \pi^+\pi^-\pi^0)$, $P_3 = \mathcal{B}(\rho \to \pi^+\pi^-\pi^0)$, $P_4 = \phi_\rho$).

Effect	P_1 (%)	P_2 (%)	P_3 (%)	P_4 (deg)
Luminosity	0.4	0.4	0.4	–
Radiative correction	0.5	0.5	0.5	–
Detection efficiency	1.1	1.1	1.1	–
MC statistics	0.1	0.2	0.2	–
Lorentzian smearing	0.3	0.4	4.7	12
Γ_ω	0.4	0.2	13.0	8
Γ_ϕ	0.0	0.0	0.3	0
ϕ_ϕ	0.2	3.1	6.1	1
Background subtraction	0.1	0.2	7.3	2
$\omega(1680) \to \rho(1450)\pi$	0.4	2.7	30.0	0
total	1.4	4.3	34.5	15

Comparison with existing cross section data

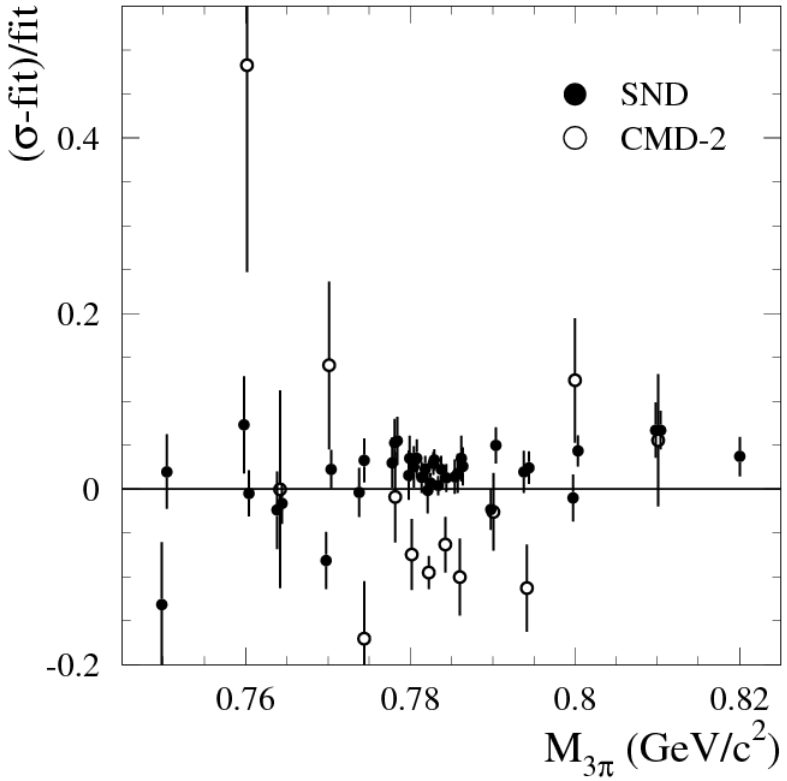

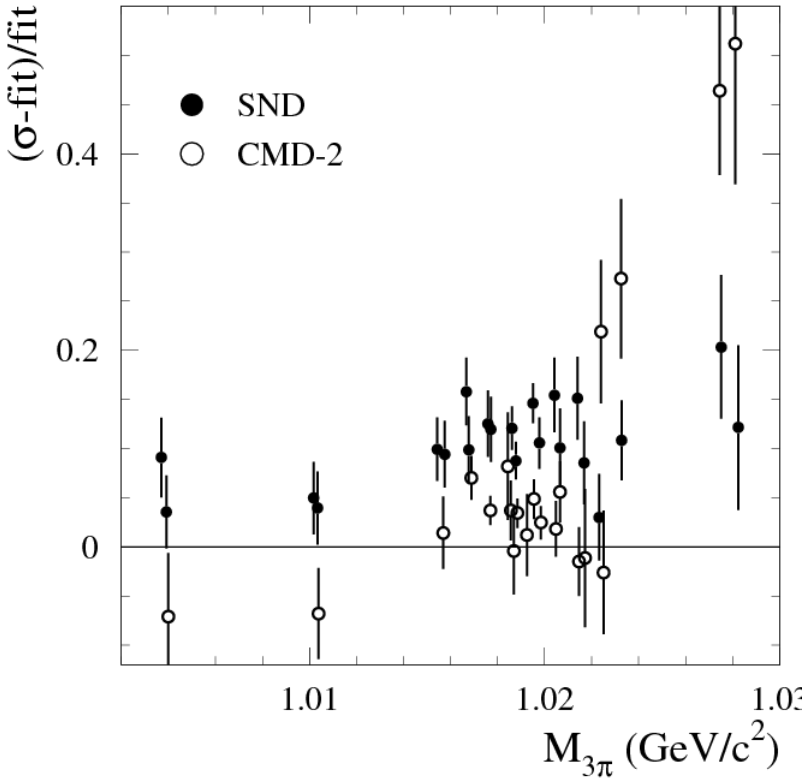

- ✓ At the ω the difference between the SND and BABAR is about 2%, well below the systematic uncertainty (3.4% for SND and 1.4% for BABAR). The CMD-2 points lie about 7% below zero. The CMD-2 statistical and systematic uncertainties are 1.8% and 1.3%, respectively. So, the difference between CMD-2 and BABAR is about 2.7σ.
- ✓ At the ϕ the CMD-2 and SND data with systematic uncertainties of 2.5% and 5%, respectively, lie about 3% and 11% higher than the fit to the BABAR data.

$e^+e^- \to \pi^+\pi^-\pi^0$ cross section below 1.1 GeV

To obtain "true" mass spectrum, unfolding is applied to the measured $M_{3\pi}$ spectrum. Similar to the previous K^+K^- and $\pi^+\pi^-$ BABAR analyses, we use the IDS (iterative, dynamically stabilized) method developed by Bogdan Malaesku.

We reweight the signal MC simulation using the results of the fit to the measured mass spectrum and obtain the folding matrix P_{ij}. The matrix is then corrected to take into account the data-MC difference in mass resolution

$$P^*_{ij} = (1-\epsilon)\sum P_{ik}G_{kj} + \epsilon L_{ij}$$

The unfolding procedure uses the transfer matrix $\boldsymbol{A_{ij} = P^*_{ij}T_j}$, where $\boldsymbol{T_j}$ is the true spectrum obtained in the fit.

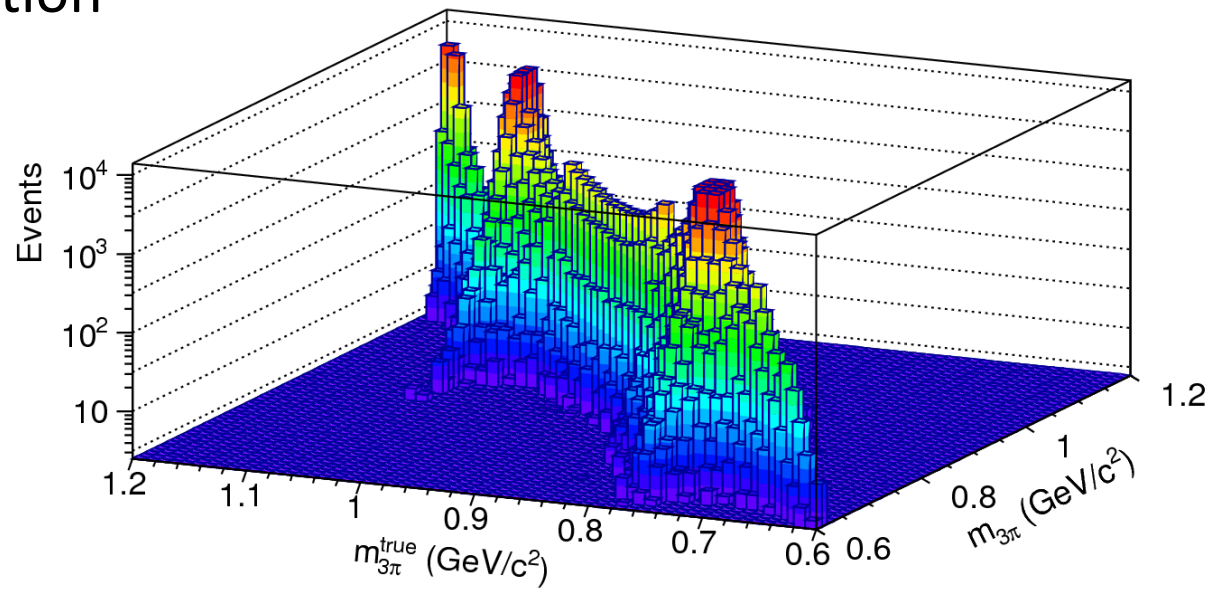

Unfolding

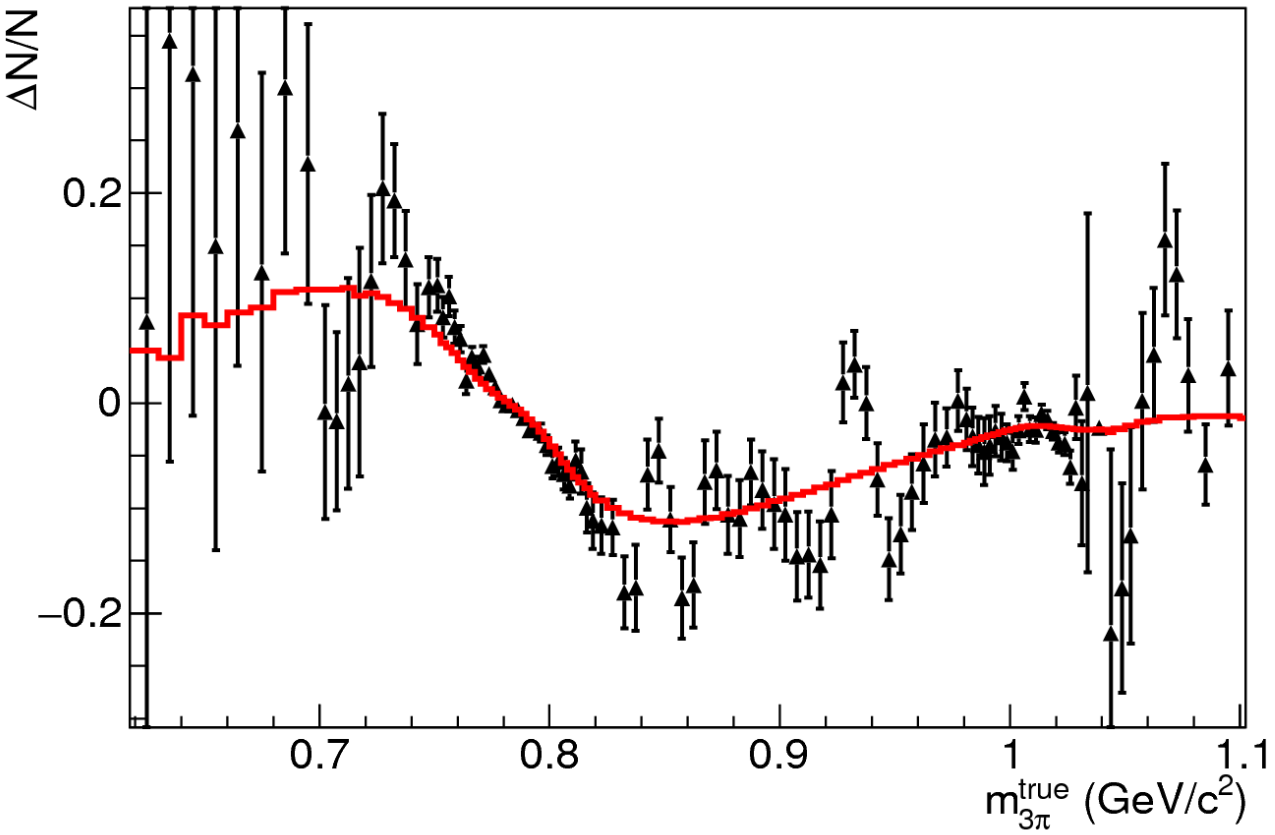

- The unfolding matrix $\widetilde{P}_{ij} = A_{ij} / \sum_j A_{ij}$ is applied to data to obtain an estimate of the true data spectrum.
- The unfolding process consists of several iteration steps.
- A regularization function is used to suppress unfolding large statistical fluctuations in data and provide the stability of the method.
- To choose parameters of the regularization functions, we use toy MC and examine two model spectra (T_i and the fit with zero $\rho \to 3\pi$ amplitude) . The regularization parameter is chosen to minimize the difference between the points and curve.

Unfolding: comparison with fit result

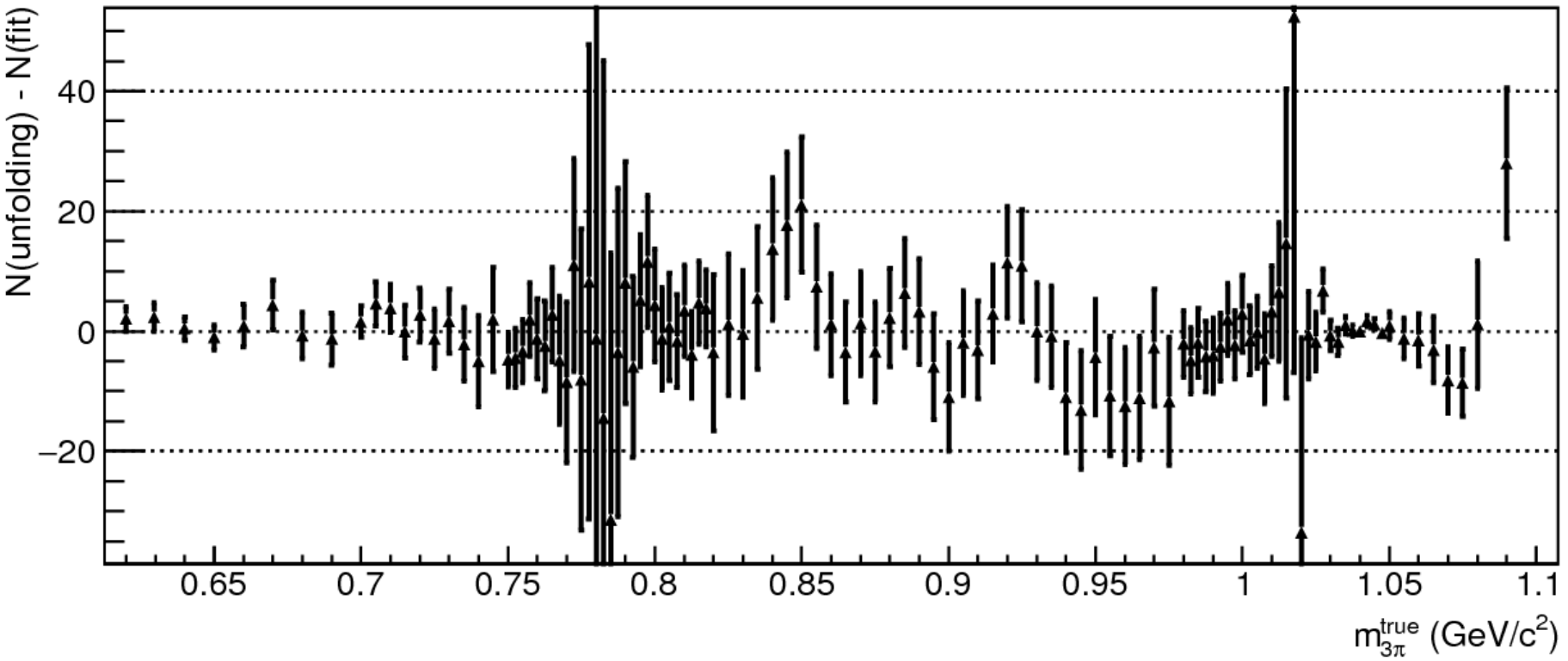

The unfolded spectrum is after the first iteration step. Further iterations do not improve the result.

Good agreement between the fit result and unfolding is seen, which confirms correctness of the model used in the fit.

$e^+e^- \to \pi^+\pi^-\pi^0$ cross section below 1.1 GeV

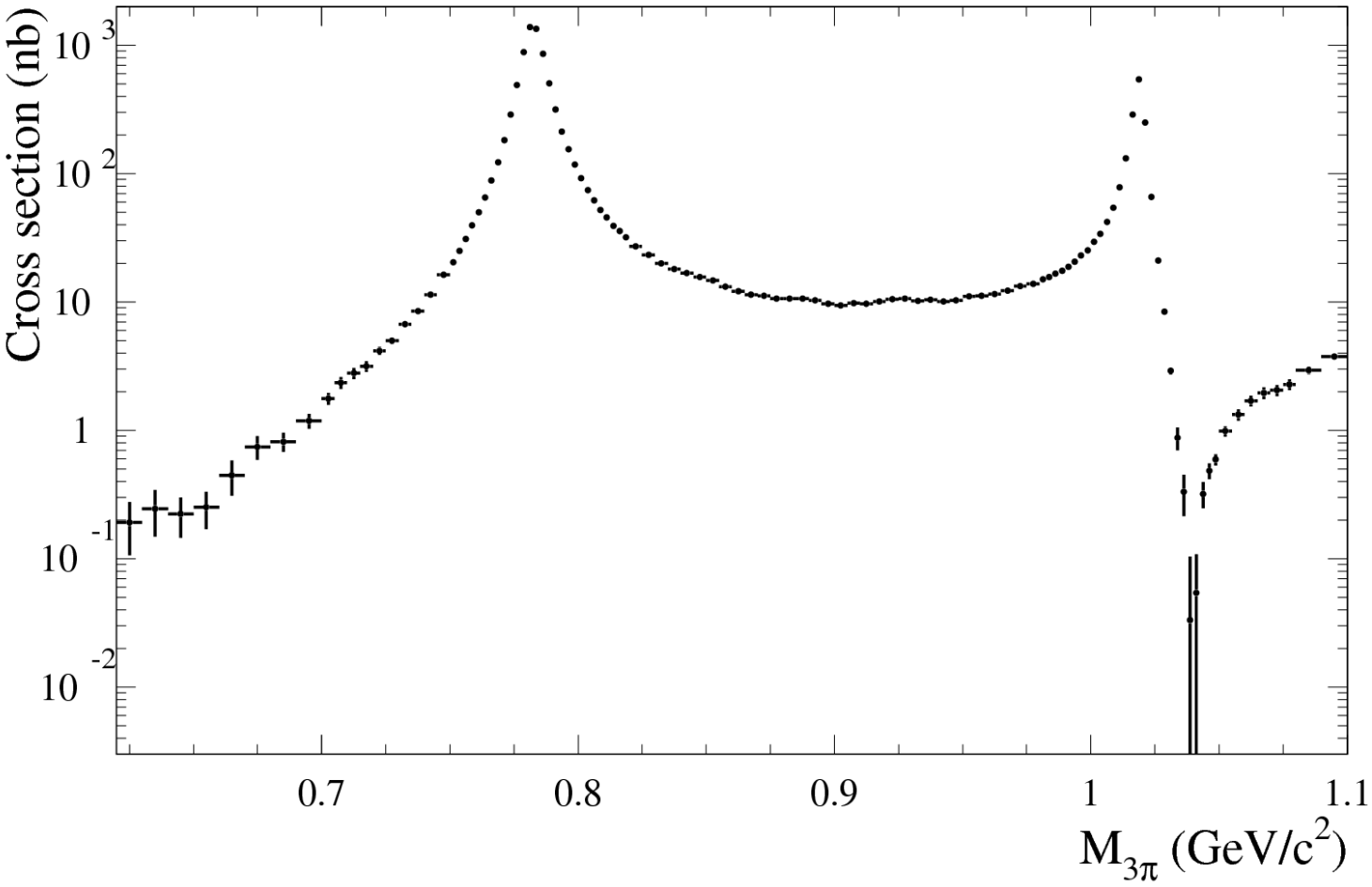

The covariance matrix is obtained from pseudo experiments (toys), where both the spectrum and the transfer matrix are statistically fluctuated.

Systematic uncertainty

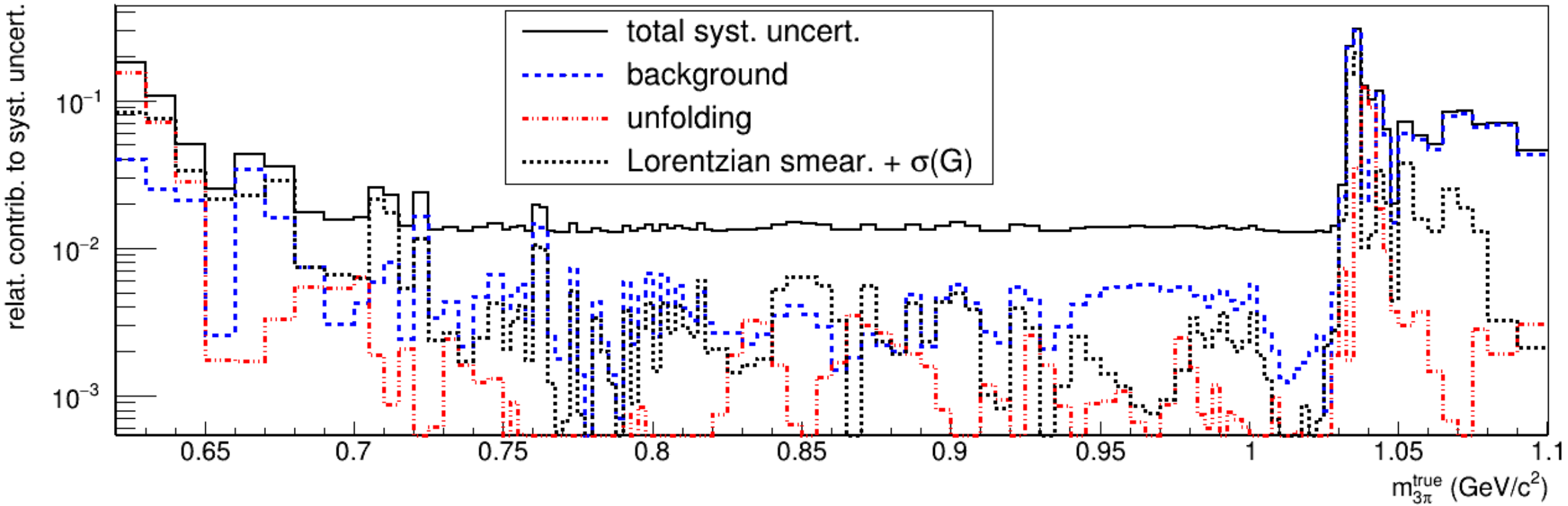

- Between 0.7 and 1.03 GeV the systematic uncertainty is dominated by the uncertainties in the luminosity, radiative correction and detection efficiency (1.3%) and is independent of mass.
- Below 0.65 GeV the largest contribution comes from the unfolding procedure, while above 1.03 GeV from the FSR background.

$e^+e^- \to \pi^+\pi^-\pi^0$ cross section above 1.1 GeV

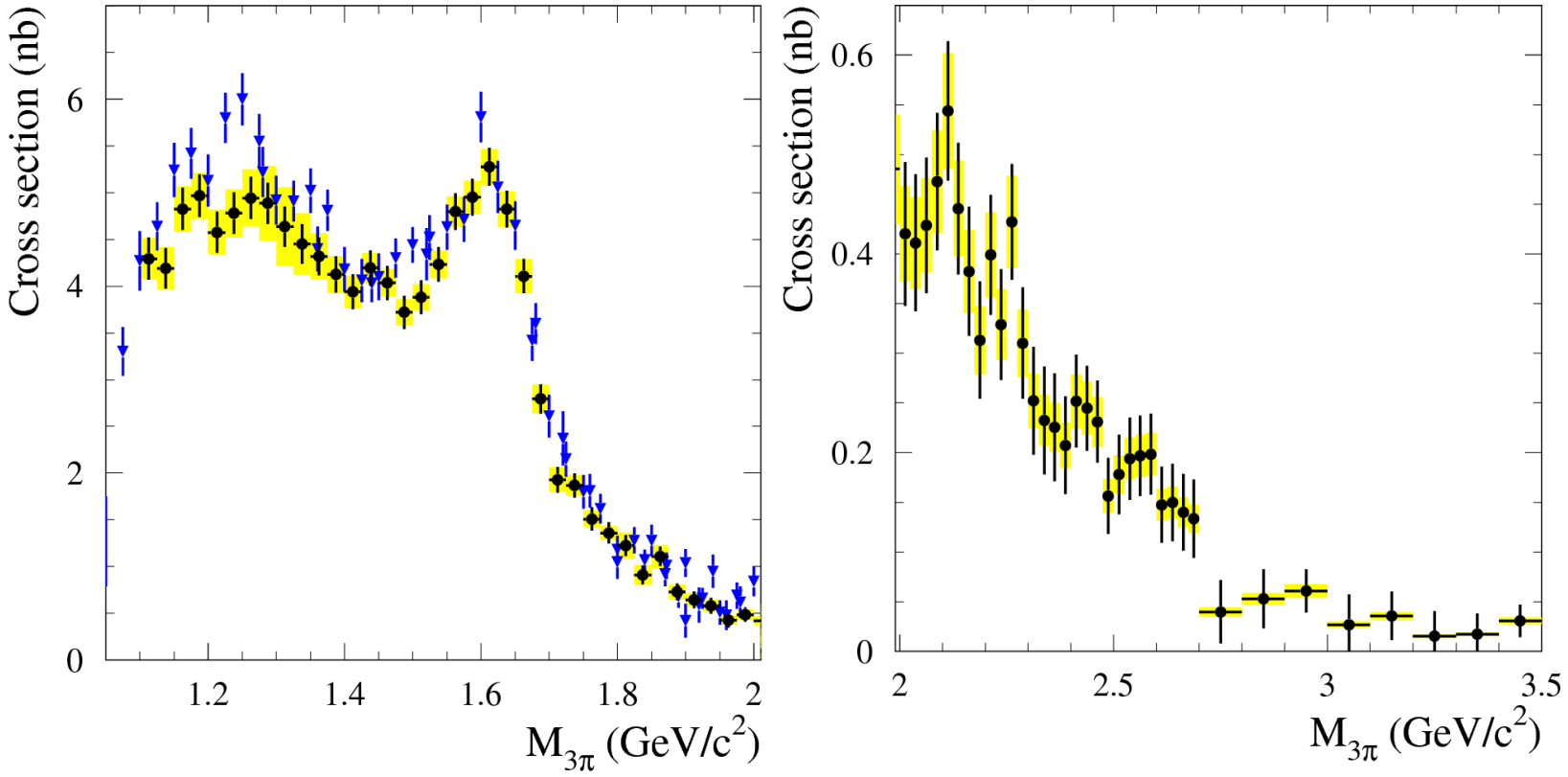

Above 1.1 GeV the resolution effects distort the 3π mass spectrum insignificantly. The toy MC study shows that the difference between the true and "measured" spectra does not exceed 1%.

The systematic error includes uncertainties in the integrated luminosity (0.4%) and radiative correction (0.5%), the statistical (0.3–2.4%), systematic (1.7–1.8%), and model (1.5%) uncertainties in the detection efficiency, and the uncertainty associated with background subtraction (3–15%).

The sizable difference between the SND and BABAR measurements is observed near 1.25 GeV and 1.5 GeV.

$e^+e^- \to \pi^+\pi^-\pi^0$ contribution to a_μ

$$a_\mu = \frac{\alpha^2}{3\pi^2}\int_{m_\pi^2}^{\infty}\frac{K(s)}{s}R(s)\,ds,\; R(s) = \frac{\sigma_0(e^+e^- \to \text{hadrons})(s)}{4\pi\alpha^2/s}.$$

$$\sigma_0(e^+e^- \to \pi^+\pi^-\pi^0)(s) = \sigma_{3\pi}(s)|1-\Pi(s)|^2$$

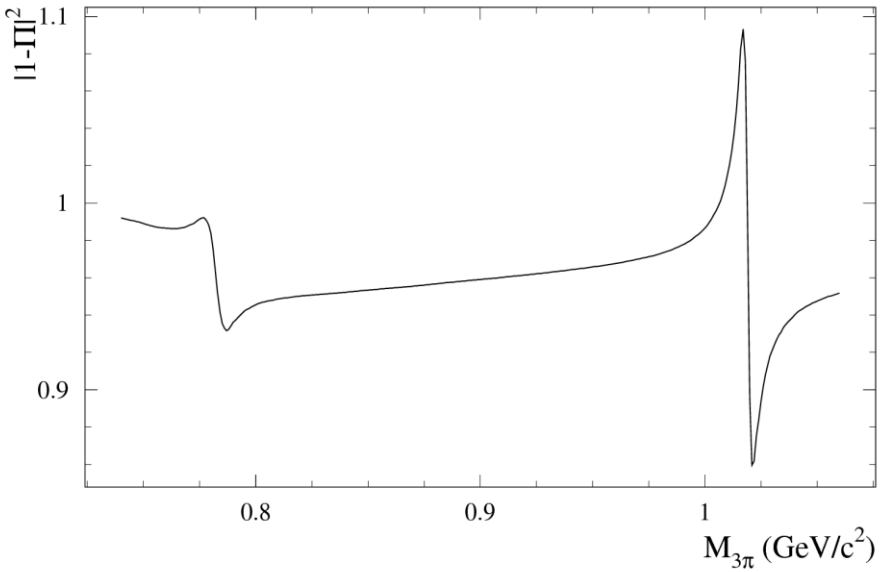

A strong s-dependence of the vacuum polarization factor leads to an additional systematic uncertainty in $a_\mu^{3\pi}$. The main contribution comes from the mass-scale uncertainty. The difference in the energy scales between SND+CMD2 and BABAR of 0.2 MeV leads to 0.2% error in $a_\mu^{3\pi}$

$e^+e^- \to \pi^+\pi^-\pi^0$ contribution to a_μ

$M_{3\pi}$ GeV/c^2	$a_\mu^{3\pi} \times 10^{10}$
0.62–1.10	$42.91 \pm 0.14 \pm 0.55 \pm 0.09$
1.10–2.00	$2.95 \pm 0.03 \pm 0.16$
< 2.00	$45.86 \pm 0.14 \pm 0.58$
< 1.80[1] DHMZ	$46.21 \pm 0.40 \pm 1.40$
< 1.97[50] KNT	46.74 ± 0.94
< 2[51] Y	44.32 ± 1.48

Uncertainty in $a_\mu^{3\pi}$ is improved by a factor of 2.

$J/\psi \to \pi^+\pi^-\pi^0$ decay

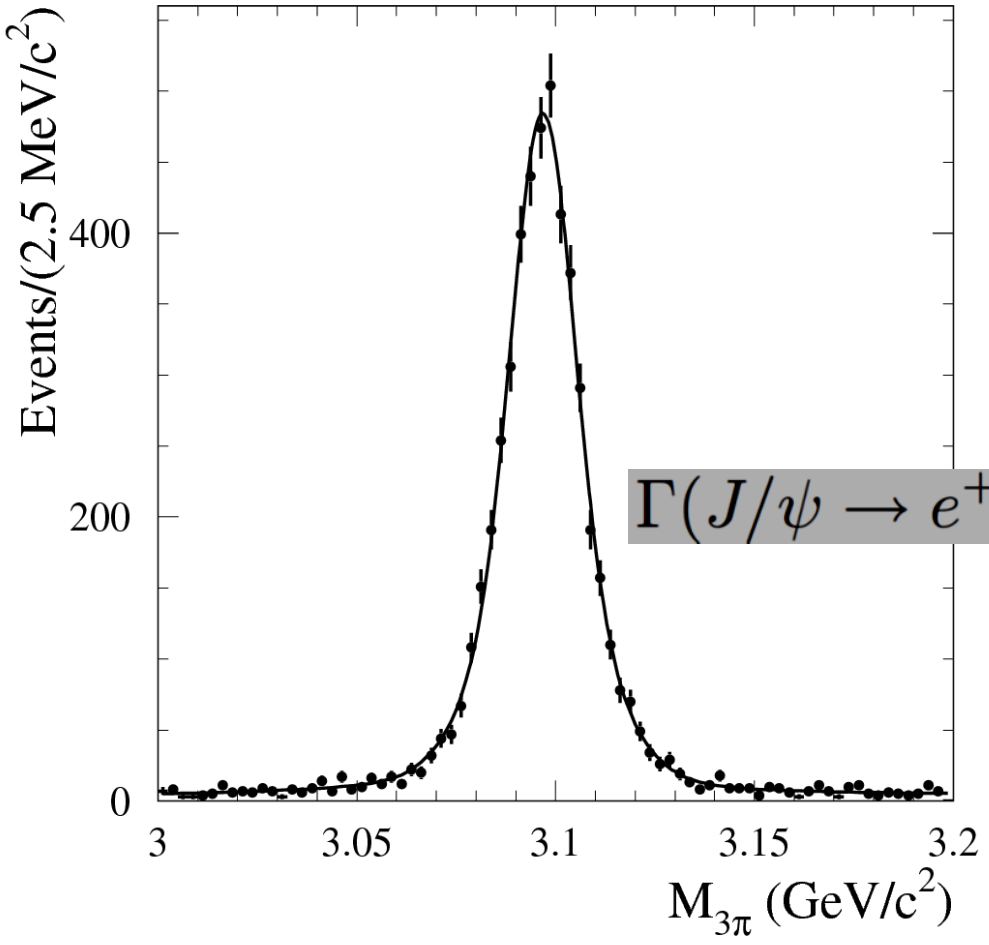

$$\frac{\mathrm{d}\sigma(s,\theta)}{\mathrm{d}\cos\theta} = \frac{12\pi^2\Gamma(J/\psi \to e^+e^-)\mathcal{B}(J/\psi \to 3\pi)}{m_{J/\psi}s} W(s, x_{J/\psi}, \theta)$$

$$N_{J/\psi} = 4921 \pm 74$$

$$\sigma_s^2 = 1.8 \pm 2.6\ \mathrm{MeV}^2/c^4$$

$$M_{J/\psi} = 3.0962 \pm 0.0002\ \mathrm{GeV}/c^2 \quad -(0.7 \pm 0.2)\ \mathrm{MeV}/c^2$$

$$\Gamma(J/\psi \to e^+e^-)\mathcal{B}(J/\psi \to 3\pi) = (0.1248 \pm 0.0019 \pm 0.0026)\ \mathrm{keV}$$

$$\mathcal{B}(J/\psi \to 3\pi) = (2.265 \pm 0.034 \pm 0.062)\%$$

PDG $(2.10 \pm 0.08)\%$

BESIII $(2.137 \pm 0.064)\%$

Summary

- The cross section for the process $e^+e^- \to \pi^+\pi^-\pi^0$ has been measured by the BABAR experiment from the 0.62 to 3.5 GeV, using the ISR method. The cross section is dominated by the ω and ϕ resonances. Near the maxima of these resonances, it is measured with a systematic uncertainty of 1.3%.
- The leading-order hadronic contribution to the muon magnetic anomaly, calculated using the measured $e^+e^- \to \pi^+\pi^-\pi^0$ cross section from threshold to 2.0 GeV, is $(45.86 \pm 0.14 \pm 0.58) \times 10^{-10}$. Our value is in reasonable agreement with the calculations based on previous $e^+e^- \to \pi^+\pi^-\pi^0$ measurements but has better (by a factor of about 2) accuracy.

Summary

- From the fit to the measured 3π mass spectrum in the process $e^+e^- \to \pi^+\pi^-\pi^0\gamma$ we have determined the resonance parameters

$$\begin{aligned}
\Gamma(\omega \to e^+e^-)\mathcal{B}(\omega \to \pi^+\pi^-\pi^0) &= (0.5698 \pm 0.0031 \pm 0.0082)\ \text{keV}, \\
\Gamma(\phi \to e^+e^-)\mathcal{B}(\phi \to \pi^+\pi^-\pi^0) &= (0.1841 \pm 0.0021 \pm 0.0080)\ \text{keV}. \\
\mathcal{B}(\rho \to 3\pi) &= (0.88 \pm 0.23 \pm 0.30) \times 10^{-4}, \\
\phi_\rho &= -(99 \pm 9 \pm 15)^\circ.
\end{aligned}$$

- The significance of the $\rho \to 3\pi$ decay is found to be greater than 6σ.
- For the J/ψ resonance we have measured the product

$$\Gamma(J/\psi \to e^+e^-)\mathcal{B}(J/\psi \to 3\pi) = (0.1248 \pm 0.0019 \pm 0.0026)\ \text{keV},$$

and the branching fraction $B(J/\psi \to 3\pi) = (2.27 \pm 0.07)\%$.